SCOUR AROUND RIVER CROSSING PILE FOUNDATIONS

A Thesis Submitted

in Partial Fulfillment of the Requirements

for the Degree of

Master of Technology

by

PRASHANT MAMGAIN

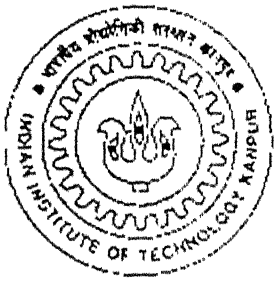

to the

DEPARTMENT OF CIVIL ENGINEERING

INDIAN INSTITUTE OF TECHNOLOGY KANPUR

MAY-2001

CERTIFICATE

It is certified that the work presented in this thesis entitled **"Scour around river crossing pile foundations"** by **Prashant Mamgain,** has been carried out under our supervision in partial fulfillment of the requirements for the award of M.Tech. Degree in Civil Engineering. This thesis is a record of bonafide work carried out in the Department of Civil Engineering, I.I.T. Kanpur during the year 2000-2001 and this work has not been submitted elsewhere for a degree.

Dr. T. Gangadharaiah

Professor

Department of Civil Engineering

Indian Institute of Technology,

Kanpur.

Dr. P.K. Basudhar

Professor

Department of Civil Engineering

Indian Institute of Technology,

Kanpur.

May, 2001

Dedicated

my teachers

ABSTRACT

In this thesis, an effort has been made to study experimentally the erosion around river crossing pile foundations under different flow conditions that may exist in the field.

All the experiments were conducted in a hydraulic flume (length-8m, width-0.4m and depth-0.6m). As there are many parameters which have direct influence on the scouring around pile foundation, it is very time consuming to study their effects varying all of them. As such, depending on the conditions either two or all of the following parameters have been varied during the conduct of the experiments. These are number of piles (maximum four), pile diameters, their spacings, arrangements, position of pile cap with respect to bed level, flow-depth, discharge, piles embedment depth below the bed level and Froude number.

Based on the experimental data points, equations for predicting the scour depth ratio as a function of Froude number and embedment depth or flow depth ratio have been suggested. Method of least square error has been used for the same.

Using simplifying assumptions an attempt has been made to develop a model for theoretical predictions of scour depth. Comparison of the experimental results and theoretical predictions shows excellent agreement for embedment depth ratio greater than two.

It has been found that for a group of four piles, square pattern of arrangement is superior to that of diamond pattern, i.e. for square pattern, erosion of sediment around piles is less. Pile cap position at a depth equal to the diameter of the piles below the ground level causes least erosion.

Acknowledgments

I feel highly indebted to my thesis supervisors Prof. P. K. Basudhar and Prof. T. Gangadharaiah for their most efficient and invaluable guidance at every stage of my thesis work. I am enriched with the practical side as well as theoretical side of the work through their scholarly guidance, constructive suggestions, critical comments and detailed instructions at every stage.

I would like to express my deep sense of gratitude to my respected Professors Dr. M. R. Madhav, Dr. N. S. V. Kameswara Rao, Dr. Sarvesh Chandra, Dr. P. K. Basudhar and Dr. Umesh Dayal for giving me an exposure and professional knowledge in the field of Geotechnical engineering.

I gratefully acknowledge the kind help, guidance and suggestions provided by Shri S. M. Ali Jawaid, Asstt. Prof. S. R. Chaurasia and Dr. Baldev Setia for my thesis work.

The help rendered by Mr. Kalyan Das, Mr. P. Jagannathan, Mr. Manoj Kumar, Mr. J. P. Pandey, Mr. Sitaram, the members of Hydraulics lab and Mr. R. P. Trivedi, Mr. A. K. Srivastava, Mr. Gulabchand, the members of Geotechnical Engineering laboratory were deeply acknowledged.

I sincerely acknowledge with respect and gratitude the kind hospitality and concern of Mrs. Basudhar, Mrs. Gangadharaiah and other family members during my several sittings at their house in connection with this programme. All were concerned about making my stay very homely here in I.I.T. Kanpur.

I am thankful to Neelam Srinivas, Meenu Kapil and Sunil Pandey for their valuable suggestions and help for my thesis.

Special thanks to my classmates Motilal, Gireesh, Sreedhar, Shekhar, Ranjan and Ramaprasad and my junior students of Geotechnical engineering group, who made my stay at I.I.T. Kanpur a pleasant one.

I am thankful to my friends Shailendra Tripathi, Chandrashekhar, Jatin, Praveen and Santosh for their constant encouragement during my Bachelor and Master's degree programme.

Finally I would like to express my gratitude to my parents and family members for their encouragement to do postgradute studies and their support at all the times.

Prashant Mamgain

CONTENTS

LIST OF FIGURES

LIST OF TABLES

LIST OF SYMBOLS

β	Exponent of D for pier size effect
ρ	Unit weight of water
σ_g	Geometric standard deviation
ρ_s	Unit weight of sand
γ_s'	Submerged density of soil
B	Channel width
C_D	Drag coefficient
D	Diameter of pile
d_{50}	Size for which 50% of the sediment by weight is finer
d_m	Mean size of the sediment in mm
D_p	Diameter of pier mounted on pilecap
D_{sc}	Scour depth measured below the water surface
f	Lacey's silt factor
F_r	Froude number
F_R	Modified Froude number
F_s	Soil resisting force
F_w	Force due to water current
G_l	Grip length at the failure condition
h	Flow depth
H_E	Embedment depth of pile below the sediment bed level
H_m	Lacey's regime depth
h_s	Maximum scour depth with respect to original bed level
K_d	Sediment size multiplying factor
K_p	Coefficient of passive earth pressure
Q	Design flood discharge in m^3/sec
q	Discharge intensity

S	Center to center spacing between piles
t	Thickness of pile cap
U	Mean velocity of flow
w_l	Weight of the super structure
w_s	Weight of pier
y	Distance of F_w from foundation base
Y	Position of pile cap with r. t. bed level

Chapter I

INTRODUCTION

1.1 General

Scour around foundations of canal, river and ocean structures poses serious challenge to civil engineers. Excessive scour in-front and deposition of bed load sediment behind the base of these structures can lead to instability and their eventual collapse. Even though the phenomenon has been observed quite early by the investigators but serious investigations for qualitative and quantitative estimation of the same started with the pioneering work of Lacy (1939), Inglis et. al. (1939) and Kennedy (1963). Since then many investigators have contributed significantly in this direction.

The process of scour and deposition of material around the foot of a bridge pier on the alluvial bed by flow as it encounters the foundation structures is called local scouring. The basic cause of the local scour is the hydrodynamic phenomenon in the form of horseshoe vortex, which develops at the leading edge of the pier junction with bed. Experimental and observational studies on the process of scour and deposition caused by the flow around bridge piers and piled foundations have been made by Tison (1940), Laursen and Toch (1956), Chabert and Engeldinger (1956), Larras (1963), Neill (1964), Paintal and Garde (1965), Shen and Schneider (1970), Melville (1975), Baker (1979,80,81), Raudviki (1990), Garde and Kothyari (1995), Sheppard et. al. (1998). They have contributed towards the prediction of scour depth under different conditions.

1.2 Brief Literature Review

A brief literature review of these studies are presented as follows:

1.2.1 Mechanism of scour

The process of scour around river structure such as bridge piers etc. involves lot of complexities of the 3-dimensional flow and sediment interaction. The scour, the flow pattern and the rate of scouring change with time and continue until steady flow conditions are re-established at the equilibrium stage. Formation of local scour occurs due to adverse pressure gradient resulting in boundary layer separation of flow near the bed level at a certain distance ahead of the structure. The separated flow then coils up to form the primary vortex, also designated in case of piers as scouring horseshoe vortex. Scouring occurs if the shear stress generated by the vortex is stronger than that required for the entrainment of the bed material. The vortex together with the down-flow provides a dominating scouring mechanism.

When a cylindrical pier or pile is held perpendicular to the flow, an adverse pressure gradient in the direction of the flow develops in its vicinity of the pier and this results in separation and rolling up of the approach flow. The rolled vortex is swept downstream around the pier. This vortex is called 'horseshoe vortex'. Melville (1975) noted that, the horseshoe vortex is initially small in cross-section and is comparatively weak. With the formation of scour hole, the vortex rapidly grows in size and strength as additional fluid attains a downward component and the strength of the down-flow increases. The down-flow acts somewhat like a vertical jet in eroding the bed. As the scour hole enlarges, the circulation associated with the horseshoe vortex increases, due to its expanding cross-sectional area, but at a decreasing rate, with the rate of increase being controlled by the quantity of fluid supplied to the vortex via the down-flow ahead of cylinder. This in-turn is determined by the discharge of the approach flow or for a particular flow depth and width, by the magnitude of the velocity of the approach flow. The magnitude of the down-flow near the bottom of the scour hole decreases as the depth of the hole increases. Hence the rate of erosion decreases. The armour coat, if present, helps to limit erosion. At a certain stage equilibrium is reached. The combination of temporal mean bed shear and the turbulent agitation near the bed becomes incapable of removing further bed material from the scour area ahead of the cylinder and in the lower

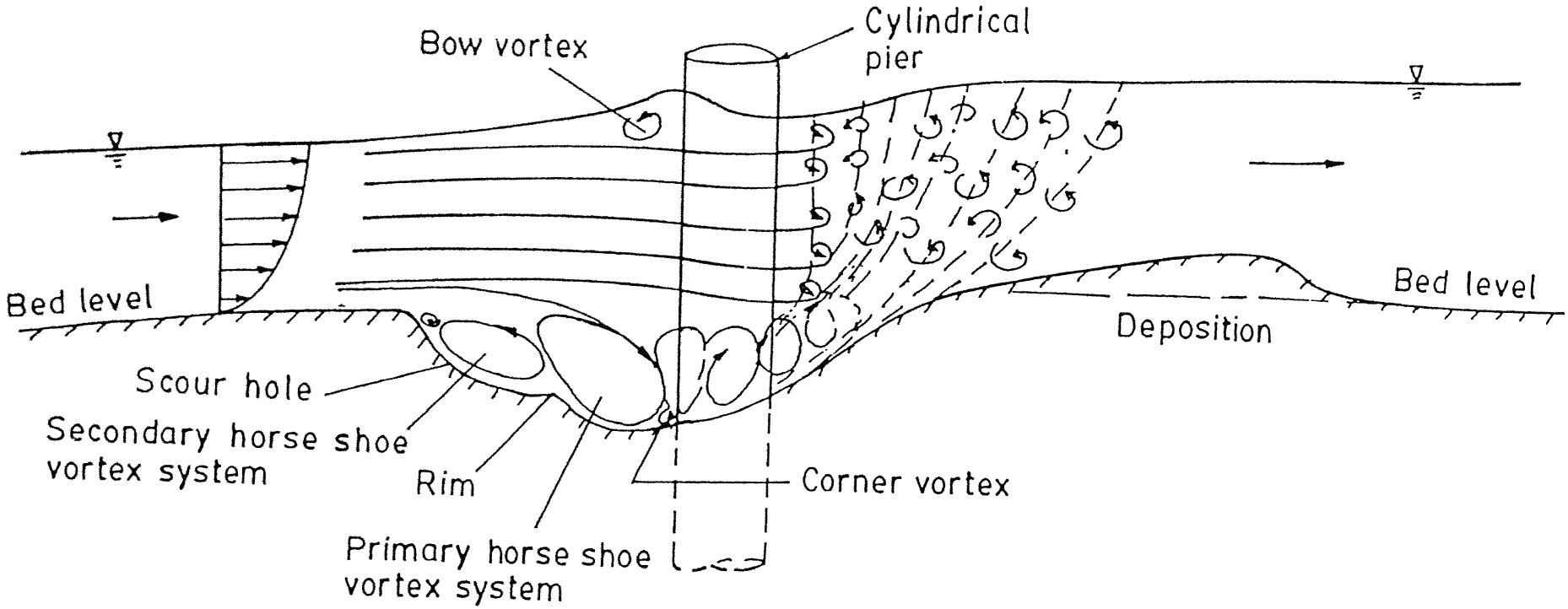

Fig. 1.1 Horseshoe Vortex on mobile bed : Longitudinal sectional view

portion of the scour hole. Hence equilibrium is a condition at which the depth of scour ahead of the cylinder is just sufficient so that the magnitude of the vertically downwards flow ahead of the cylinder can no longer dislodge surface grains at the bed. The horseshoe vortex and scouring phenomenon around cylindrical pier is shown in Fig. 1.1.

A number of investigators like Larsen and Toch (1956), Roper et al. (1967), Baker (1981), Kothyari (1989), Muzzamil and Gangadharaiah (1995) considered the horseshoe vortex as the basic cause of local scour.

1.2.2 Scour depth predictions

Estimation of correct depth of scour at the bridge below the ambient stream bed is very important since that determines the depth of foundation for the pier. Which is very much important for the geotechnical aspect of design. Based on different approaches, many formulae have been proposed for the prediction of local scour depth at bridge piers. Some of them are presented here.

Inglis et al. (1939) carried out model studies on piers in connection with the Hardinge bridge works over river Ganga. They found that scour depth could be expressed as :

$$\frac{h_s}{D} = 2.32\left[\frac{q^{2/3}}{D}\right]^{0.78}$$

Where h_s = scour depth measured below the sediment bed level

D = diameter of the pier

q = discharge intensity in m^3/sec/m.

A major disadvantage of this relation is the combination of undisturbed water depth and scour depth. The formula was later modified using regime depth relations by Blench (1962) and Arunachalam (1967). Inglis (1949) based on the analysis of scour data on 17 bridges in the Indo-Gangetic plains proposed a formula for the scour depth,

$$D_{sc} = 2\ H_m$$

Where H_m is known as Lacey's regime depth given as:

$$H_m = 0.47\left[\frac{Q}{f}\right]^{1/3}$$

Where ,

D_{se} = scour depth measured below the water surface = $(h+h_s)$

f = Lacey's silt factor = $1.76\sqrt{d_m}$

d_m = mean size of the sediment in mm

Q = design flood discharge in m^3/sec

h = depth of flow

This is popularly known as Lacey-Inglis method of estimating scour depth and is recommended for use by Indian railways and Indian road congress. This method is purely empirical in nature and gives combined scour caused due to flow modification by introduction of a pier, flow constriction due to guide bunds, and flow concentration due to non-uniform distribution of flow. It is obvious from the formula, that the pier geometry and the flow depth are unimportant. This approach does not reveal the internal mechanism involved in the scouring pattern.

The regime equation originally derived for straight reaches of channels in equilibrium for parallel flow conditions are not applicable to flow conditions at bends and obstructions, where the flow is mainly characterized by large scale curvatures, separation, vortex formation, macro-turbulence and energy dissipation.

1.2.3 Scour around piled foundation

Till now scouring around piers has been thoroughly investigated than that of pile groups. Useful insight to this aspect of local scour is provided by an investigation by Hannah (1978), who studied local scour at groups of cylindrical piles with steady uniform flow and clear water conditions.

For scour at piled foundations, where the pile cap is clear of the water surface, Hannah (1978) found that the maximum scour depth is closely related to the dimension of the pile group as a hole, as seen from the upstream. He recommended that a single line of piles

should be used in preference to piers for angle of attack greater than 8 degrees. A series of tests was first performed on single piles with a pier (length : width = 6 : 1) to provide a basis against which pile group scour could be evaluated. Pile group of various spacings and with different angle of attack was then investigated for one flow conditions. The sediment used in all tests had a d_{50} = 0.75 mm and standard deviation (σ_g) = 1.32. Tests showed that scour depths were 80% of equilibrium scour depths after seven hours. Further, after seven hours, only minor changes occurred in scour and deposition patterns.

Raudviki (1990) explained the scouring pattern for the two piles in series and in transverse direction. When the two piles are in series and are in contact, the scour depth at the front pile was same as that for the single pile. But with increasing separation, the front pile experiences the reinforcing effect which reaches a maximum value at a/b = 2.5 and is evident until a/b = 11. Where a is the center to center spacing between piles and b is the common pile diameter. For larger spacings, the scour depth is the same for a single pile. With larger separation (a/b=10) between the piles, bed level increases as some of the material from the front hole is deposited between the piles. At a spacing of a/b = 10, the scouring in front of second pile is balanced by deposition from the front scour hole. For larger spacings, the reinforcing effect at the front pile is weak and disappears completely as the bed profile assumes that arising from scour at a single pile. For the piles in transverse direction, at close spacings, (a/b= 2), the increased scouring results from the increase in effective pile diameter. At a/b =2, separate horseshoe vortices form between the piles, these are compressed thus creating higher velocities and greater scouring potential which reduces as a/b increases.

Melville (1998) shows that piers founded on a slab footing (wider than the pier) caisson or pile cap, the footing, capping or caissons with the top below the general bed level can be effective in reducing the local scour depth by interception of the downflow. However, if the top of the wider foundation element comes to bed level, or even above, the scour depth is increased.

Melville conducted the experiments for the following four cases:

1. Top of footing below the scour hole.
2. Top of the footing within the scour hole below the general bed level.

3. Top of the footing above the general bed level.
4. Where the footing is at or above the water surface level.

He concluded that for the first case, when the footing, cap or caissons buried below the scour hole base, local scour has no effect due to footing. While in the second case, local scour is reduced due to the interception of the down-flow. For the third case, scour depth increases for a pier founded on a large size caisson. But for the fourth case, the maximum local scour occurs, when the top of the caisson or pile cap is at the water surface level.

1.2.4 Effect of pier shapes and sizes

Bridge piers are constructed in a variety of different sizes and shapes. Among all, circular piers are defined as the standard pier shape. The effect of pier size on scour depth is proportional, i.e. larger the size, more is the equilibrium scour depth. But opinions presented on relationship between scour depth and pier size are quite diverging. With all the other factors being constant, the scour depth varies as D^{β}, where D is the size or width of the pier and $0.5 \leq \beta \leq 1.0$. Laursen and Toch (1956) design curves corresponds to $\beta = 0.7$ for the equation ($h_s = 1.05\ D^{\beta}h^{0.3}$), Larras (1963) suggests $\beta = 0.75$ for ($h_s = 0.75\ D^{\beta}$) and Breusers (1972) proposed $\beta = 1$ for ($h_s = 1.4\ D^{\beta}$). where h_s shows the maximum scour depth around unprotected pier.

Mostafa (1994) measured local scour depths at a variety of different uniform pier shapes all having the same projected width. Results show that the least scour depth for the same flow conditions is recorded for the circular pier. Non-uniform pier include piers with pile foundations, caissons, slab footing and tapered piles. Downward tapering piers induce deeper scour than a circular pier of the same width, and vice versa. The general conclusion is that the blunter the pier the deeper the local scour. It is because, the frontal area of the pier facing the flow increases for a blunt rather than a streamlined shape.

1.2.5 Influence of constriction ratio

The constriction ratio, defined as the ratio of the width of the flume to the size of the pier, (B/D), influences the equilibrium scour depth at the piers. Shen et al (1969) suggest that, for

clear water experiments, the flume width should be atleast eight times the diameter or size of the pier. The same ratio for live bed scour should be atleast 10 times the pier size (Chiew 1984). A flume width smaller than this, is likely to reduce the scour depth as the bed features are likely to be modified as they move through the constriction.

1.2.6 Influence of sediment size

Ettema (1980) and Chiew (1984) studied the influence of sediment size on scour depth at circular piers for uniform sediments for clear water flows and live bed scour respectively. Their data show that the equilibrium scour depth increases with the relative sediment size (D/d_{50}) upto $D/d_{50} = 50$. For ($D/d_{50} > 50$), which is the case of most of the practical situations, H_{sm} is independent of the sediment size. Ettema explained that the reduction in scour depth for relatively large sediments were due to large particles impending the erosion process at the base of the scour hole and dissipating some of the flow energy in the erosion zone.

For non-uniform sediments ($\sigma_g \geq 1.3$) a process known as armouring occurs in the scour hole. Where σ_g represents geometrical standard deviaton obtained from the logarithmic-probability distribution graph. The differential mobility in a mixture of particles of different diameters is responsible for armouring or paving of the channel bed. Armour layer formation in non-uniform sediments leads to reduced scour depths (Dongal,1994; Raudkivi et. al.,1977; Wong,1982; see Juyal,2000). The effective size of non-uniform sediment can be defined as the size of uniform material which gets scoured at the same rate as the non-uniform material under the given conditions.

Data by Baker (1986) for pier scour in graded sediments under live bed conditions show that sediment gradation effects are considerably reduced at higher flow intensities. Melville (1992) plotted data of Wong (1982) under clear water conditions for abutments which showed dramatic decrease in scour depth for widely graded sediments. Melville (1997) plotted pier and abutment data in terms of the sediment size multiplying factor, K_d, which is defined as the ratio of the scour depth for a particular D/d_{50} to that for $D/d_{50} \geq 50$.

1.2.7 Influence of flow depth

There are conflicting views on the effect of flow depth on the local scour depth. Observation show that at shallow flow depths, the local scour at piers increases with flow depth but as the water depth increases, the scour depth becomes almost independent of flow depth. This trend is shown by Laursen (1963), Breusers (1977), Ettema (1980), Chiew (1982). Laursen (1963) and most researchers influenced by the regime theory state that for constant velocity, the depth of scour increases with increasing water depth. The presence of a pier causes a free surface roller around the pier and the horseshoe vortex roller at the base of the pier. The two rollers have opposite direction of rotation, Melville (1988). As long as they do not interfere with each other, the local scour depth is independent of flow depth.

1.2.8 Influence of angle of attack

The depth of local scour for all shapes of pier except cylindrical, is strongly dependent on the alignment to the flow. As the angle increases, the scour depth increases because the effective frontal width of the pier is increased. Melville (1977) observed that at a zero angle of attack the scour depth can be minimised by streamlining the pier, but this advantage disappears for angles of attack greater than 10^0.

1.2.9 Methods of reducing local scour

Scour protection devices have been classified in to following categories (Setia, 1997):

(a) Weakening of the horseshoe vortex by providing piles upstream of piers or slot in the pier.

(b) Arresting the sinking of horseshoe vortex by providing rip rap material or collar plates type of devices.

(c) Modifying the horseshoe vortex by providing delta-wing like passive device.

Setia's (1997) experiments reveal that each type of protection good for particular flow conditions. Combination of them is found to act as better scour protection aids.

1.2.10 Pile group effect on scour depth

Hannah (1978) (see Raudkivi, 1990), studied the local scour at group of cylindrical piles with steady uniform flow and clear-water conditions. Four types of mechanisms that occurs during scouring process when piles are arranged in a row, are described as follows:

(1) **Reinforcing:** It causes increased scour depths at the front pile. If the downstream pile is so placed that the scour hole overlaps, then the bed level is lowered at the rear of the upstream scour hole. It is thus easier for the flow to remove material from this hole and it deepens. As pile separation increases, the reinforcing effect reduces and disappears when the maximum bed level between the piles returns to the undisturbed bed level.

(2) **Sheltering:** The presence of an upstream pile can cause a reduction in the effective approach velocity for downstream piles. This reduction decreases the effect of the 'horseshoe vortex' and thereby reduces scour at downstream piles. A second form of sheltering occurs if material scoured from the upstream pile is deposited on the bed in front of the downstream pile. Flow is then deflected up from the bed and around the downstream pile. The strength and thus the effectiveness of the horseshoe vortex at this pile is reduced. As pile separation increases, the sheltering effect decreases.

(3) **Vortex Shedding :** Vortices shed from an upstream pile are convected downstream. When a second pile is so placed close to one of the vortex shedding paths, the vortices assists in lifting the material from the scour hole. The scouring potential of the shed vortex is a function of its convection speed and of the distance between the path and the affected pile. This effect will therefore, reduce more rapidly for piles in line and for those downstream piles placed on the paths traced by vortices shed by upstream piles.

(4) **Horseshoe vortex Compression :** when piles are placed transverse to the flow, each pile will have, except at very close spacings, its own horseshoe vortex. As pile spacing is decreased, the inner arms of the horseshoe vortices will be compressed. This causes velocities with in the arms to increase with a consequent increase in scour depths. This compression also exists for piles in staggered arrangement.

Experiments were conducted by Jones (1993) to determine guidelines for specifying the characteristic width of a pile group that is or may be exposed to the flow. He concluded that, when pile groups project above the streambed, they can be analyzed conservatively by representing them as a single width equal to the projected area of the piles ignoring the clear space between piles. Good judgement needs to be used in accounting for debris because pile groups tend to collect debris that could effectively clog the clear spaces between piles and cause the pile group to act as a much larger mass.

1.3 Motivation and Objective of the present study

Literature review indicates that most of the works are focussed on scour depth prediction due to interference of piles arranged in staggered, parallel, and tandem patterns. But there is no information regarding piles in a group arranged in either diamond or square patterns. This situation arises in the design of foundation for transmission towers built in alluvial river beds. The transmission towers consists of tower structure mounted on pile cap and pile cap supported by piles arranged in a particular pattern. Alternatively each leg of the transmission line tower may rest on an individual well. As such, there is no necessity of constructing a platform on them.

The position of pile cap and arrangement of piles are important factors for the stability of towers against the fluctuations in the bed level due to the non-uniform flow conditions in the river. The embedment depth is also an important factor for the safety of piers against overturning or failure due to increased flow in the rivers

The present study focussed mainly to find the particular arrangement of piles, suitable position of pile cap and to provide adequate embedment depth of piles with changed flow conditions, so that the safety of river crossing structures can be ensured. For this, it is necessary to estimate the scour around these structures under varying flow conditions for soils that are generally found in the river beds of the region. In this study, experiments have

been conducted with Yamuna sand with the purpose of developing a general equation for the same. Knowing the depth of scour, it is possible to predict the necessary grip length for adequate safety and stability of such foundations. Till now no information is available in literature to estimate directly the grip length as a function of scour depth, flow depth and Froude no. Thus, there is a need to develop such an expression. So, in this thesis an effort has also been made to find a rational expression based on theoretical approach and experimental observations.

1.4 Organization of Thesis

The thesis contains the following chapters:

1. Introduction and brief literature review.
2. Experimental details.
3. Experimental results and discussion.
4. Theoretical prediction and comparison with experimental results.
5. Conclusions.

Chapter II

EXPERIMENTAL DETAILS

2.1 General

The experiments were conducted in a hydraulic flume located in the Hydraulic and water resource laboratory, Department of Civil Engineering at Indian Institute of Technology, Kanpur.

Studies were made to meet the objectives as stated in the earlier sections. Experiments were planned and designed to represent different conditions that may be encountered in the field. Various parameters representing the physical model and the flow conditions were varied to investigate their influence on the overall behavior. As there are many parameters which have direct influence on the scouring of soil around pile foundation, it is very time consuming to study their effects by varying all of them. As such, depending on the conditions, either some or all of the following parameters are varied during the conduct of the experiments. These parameters are pile or pier diameter, their spacings, arrangement, position of pile cap with respect of the bed level, flow depth, discharge, pile's embedment depth below the bed level and Froude number.

In the following sections, various experimental details are described in brief.

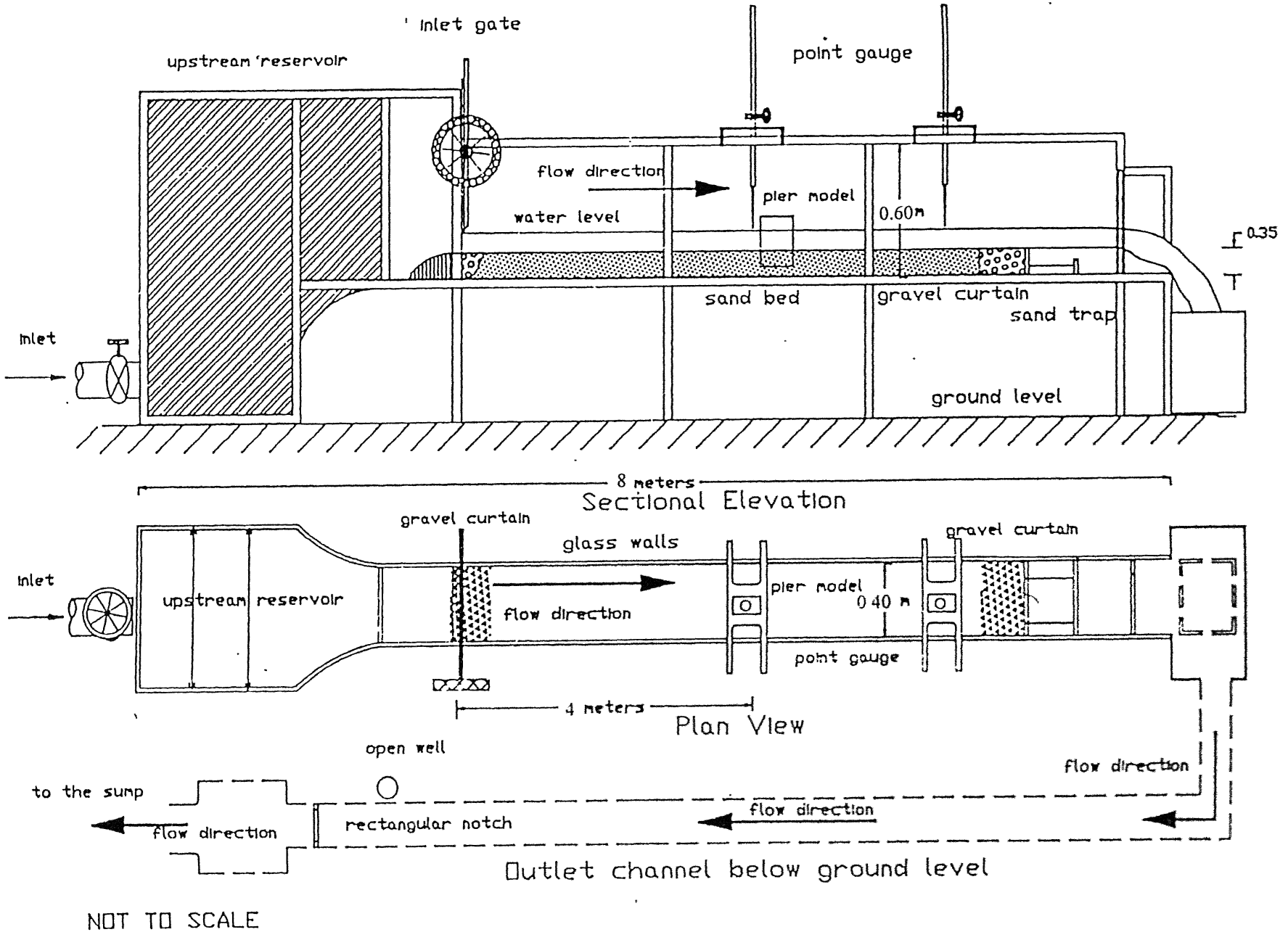

Fig. 2.1 Detailed sketch of Experimental Channel

2.2 Experimental channel

Experiments were conducted in a glass walled channel, 8.0 meter in length, 0.40 meter in width and 0.60 meter deep. The channel was filled with coarse sand (Yamuna sand, d_{50}=0.60 mm). Coarse sand bed was 0.20 meter deep and was packed with gravel curtain on upstream and downstream ends to prevent erosion of sand at the inlet and outlet during the flow of water. A sediment trap was also provided at the end of downstream gate. Depth of flow in the flume was controlled by two gates, one at the upstream and the other at the downstream of the model. The water flow was received from a overhead tank and the discharge was measured with the help of a triangular notch provided at the end of the sediment trap. The outflow was recirculated with the help of water pumps. The arrangement is shown in Fig 2.1.

2.3 Characteristics of sand

Yamuna sand passing through 2 mm. IS sieve has been used in conducting all the experiments. The particle size distribution curve for this sand is shown in Fig.2.2. The uniformity coefficient (C_u) and the coefficient of curvature (C_c) of the sand are 1.32 and 1.13 respectively. The chosen sand is categorized as poorly graded sand (SP) as per IS code. This sand has the following other properties:

d_{50} = 0.60 mm

Specific Gravity (G_s) : 2.66

Shear strength parameters of sand (Direct shear test):

Placement density = 14.38 kN/m^3

(i) Dry condition :

$\phi = 29^0$

c = 0.0

(ii) Submerged Condition :

$\phi = 28.48^0$

c = 0.0

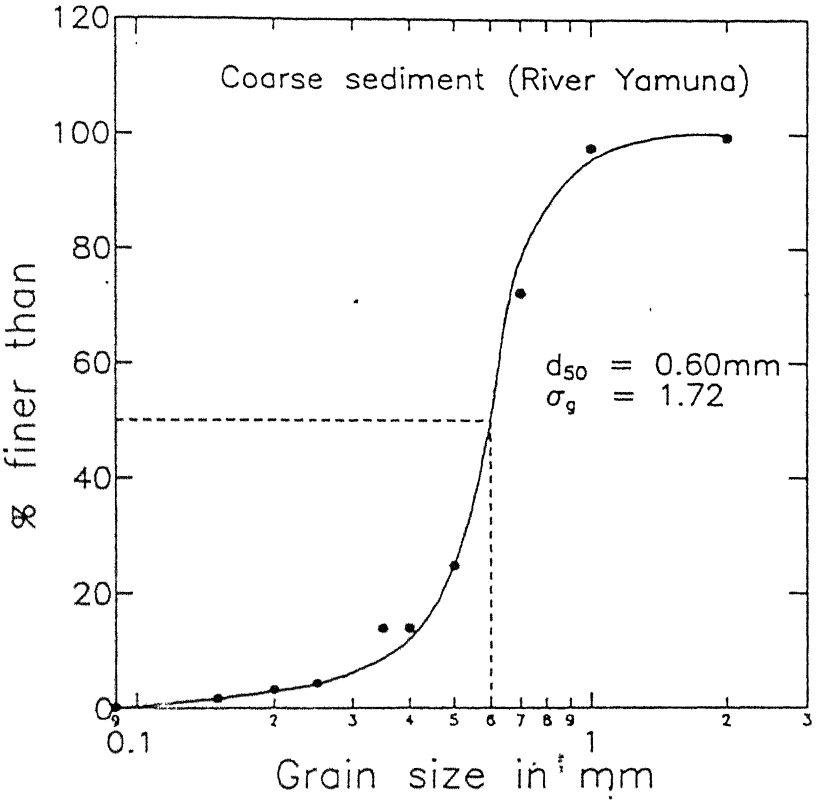

Fig. 2.2 Particle size distribution of sediments

2.4 Conditions during experiments

Experiments were conducted in the channel as described in section 2.2, under the following conditions:

1. Flow depth was maintained as constant throughout the duration of the experiment
2. Flow is considered to be uniform throughout the experiment.
3. The orientation of the model in the direction of flow for all experiments has been so maintained that the angle of attack is taken to be 0^0.
4. The interference of walls of the channel can be neglected as the aspect ratio (B/D) is greater than 5. Where D is the diameter of pile and B is width of the experimental channel.
5. Channel bed slope was negligibly small and can be considered to be horizontal.

2.5 Experimental procedure

Before starting any experiment, sediment bed had been properly leveled and bed levels were measured along the flume length at three sections, one at the test section and the others, one at 1.0 meter upstream of the test section and last one at 1.0 meter downstream of the test section. Water was allowed gradually into the flume to attain a velocity such that the particles would just start moving (except in pile's embedment depth measurement series of experiments where particles were allowed to move freely with increased discharge). The test section chosen was located at a distance of 3.0 meter from the inlet. The required conditions, like depth of flow and discharge were maintained steadily during each set of experiment.

Two types of experiments were conducted. In the first one, cylindrical model piles of different diameters (25mm, 37.5mm, 50mm, 62.5mm and 75mm) were inserted at the test section of the channel, deep in to the sand bed providing sufficient embedment depth. In the second one, model piles of diameter 25mm each, attached to pile cap (12mm thick) and a pier made up of G.I. was mounted on top of the pilecap were used. Length of pile was so chosen that it was sufficient enough not to expose the pile base at the time of maximum scour and the height of pier placed on the top of pile cap was such that the maximum flow depth used during the experiments was less than the pier height. The

A series of experiments was conducted with a PVC pipe of diameter 50 mm for measuring the embedment length at the limiting equilibrium. Length of the piles were chosen in such a way that even for the maximum possible embedment depth, the top of the piles was above the maximum water level.

2.6 Details of experiments

Experiments have been conducted under varying conditions of pile diameter, their arrangements and flow conditions. The details of the same are given as :

(A) Variation of scour depth with flow depth

This experiment is done with the help of a single pile of diameter 25mm. The flow depth (h), is varied as h = D, 2D, 3D and 3.5D for each setup of experiment where D is the diameter of pile used. Scour depth was measured after 10 hours of sustained flow.

(B) Piles without pile cap

Scour depth measurements were made for the following cases:

(a) Single pile; diameters varying from 25mm, 37.5mm, 50mm, 62.5mm and 75.0mm.

(b) Two piles of equal diameter (each 25 mm) arranged in series with a spacing of four times the diameter of the pile (D) as shown in Fig 2.3 (A).

(c) Two piles of equal diameter (each 25 mm) arranged in parallel pattern with a spacing of 4D as shown in Fig 2.3 (B).

(d) Group of four piles of equal diameter arranged in square pattern, keeping the center to center spacing of the piles as 3D, 4D, 5D and 6D respectively as shown in Fig. 2.4 (B).

(e) Group of four piles of equal diameter arranged in diamond pattern varying the center to center spacing between the piles as 3D, 4D, 5D and 6D.respectively as shown in Fig. 2.4 (A).

(f) Varying the depth of flow (h) for a single pile of diameter 25 mm by varying the flow depth to diameter ratio (h/D) = 2, 3 and 3.5 and 4 respectively.

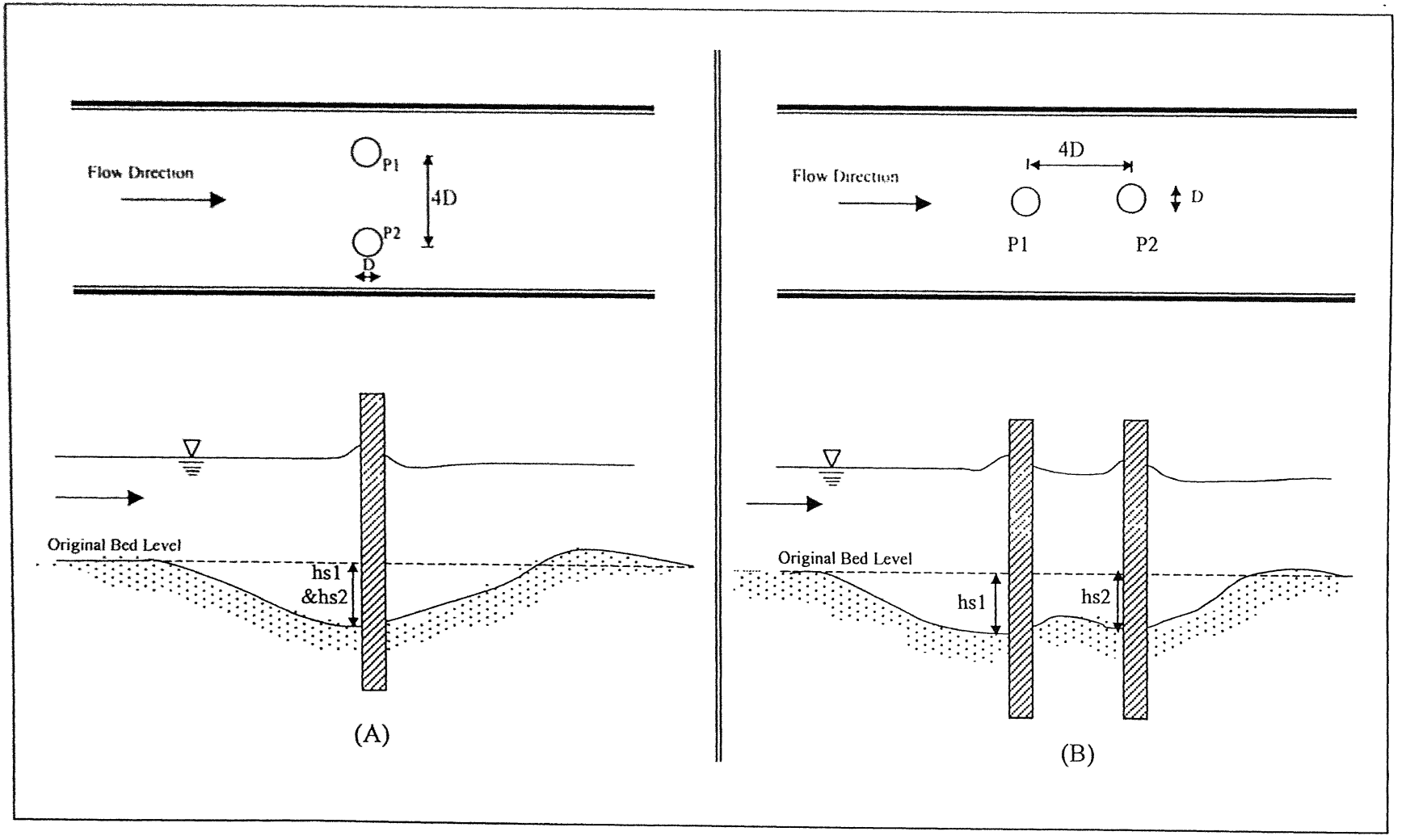

Fig.2.3 Two piles in (A) Parallel and (B) Series patterns

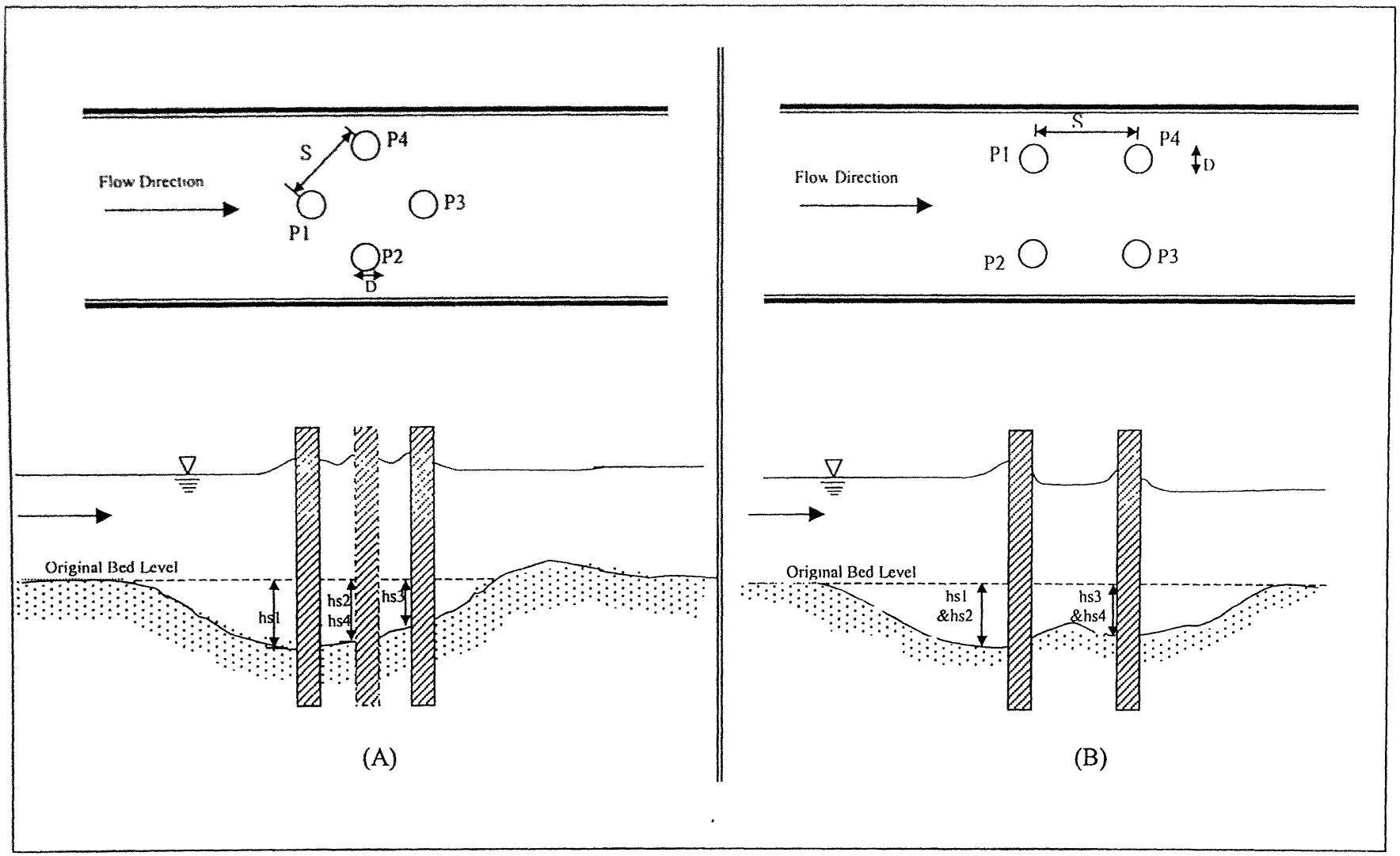

Fig. 2.4 Four piles in (A) Diamond and (B) Square pattern

(C) Piles with a pile cap

The four piles were arranged either in a square or diamond pattern with respect to the flow as shown in Fig. 2.5 with a diagonal spacing of 4D. The piles were interconnected by a pile cap. The position of pile cap with respect to the bed level was varied keeping the ratio of the height of pile cap above or below the bed level to pile diameter (Y/D) as -1, -2, 0, 1, 2, 3.

Negative sign shows the position of pile cap below the bed level and positive sign shows the position of pile cap above the bed level. Y shows the position of pile cap with respect to the bed level.

(D) Variation of embedment depth of pile with flow depth

For this series of experiment a pipe of diameter 50mm was used. Initial setup of pile before start of scouring is shown in Fig. 2.6. For each setup, embedment length of pile below the sediment bed level is varied and scour depth at which the pile failed (i.e. tilted or washed away, as shown in Fig. 2.7) is measured. Froude No. is varied with the increase of discharge and the flow depth. The embedment depth of the pile was chosen sequentially as 1.5D, 1.75D, 2.0D, 2.25D, 2.5D, 2.75D and 3.0D. Froude no. is also varied with embedment depth to cause failure of the pile. After each experiment, sediment bed level was properly leveled by taking the washed sediment back to the bed from the trap, where sediments were collected during the flow.

2.7 Scour Depth Measurements

Measurement of scour depths were made with the help of a point gauge with a least count of 0.01 cm. The area around the test section was illuminated with the help of a bulb, so that the observations can be made correctly. Measurements were made at the point of maximum scour around piles.

Each set of experiment was conducted for 600 minutes. Readings were taken at the following time intervals namely 1, 2, 5, 7, 10, 20, 30, 50, 70, 150, 200, 300, 400, 500 and 600 minutes respectively after the initiation of scouring. Scour depth was measured at that point around piles, where the maximum scour depth occurred. For measurement of scour

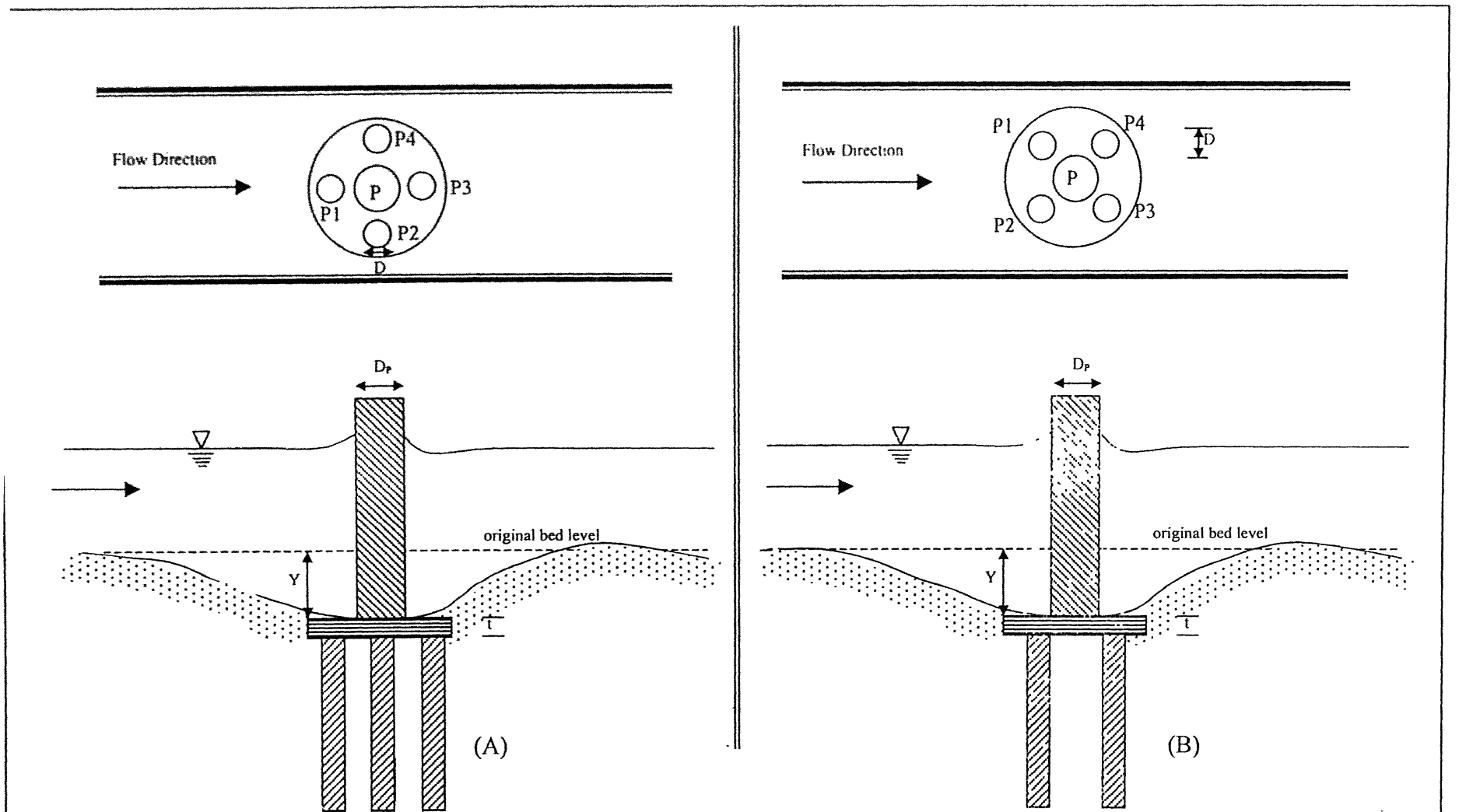

Fig. 2.5 Pier founded on piles with pile cap in (A) Diamond and (B) Square pattern

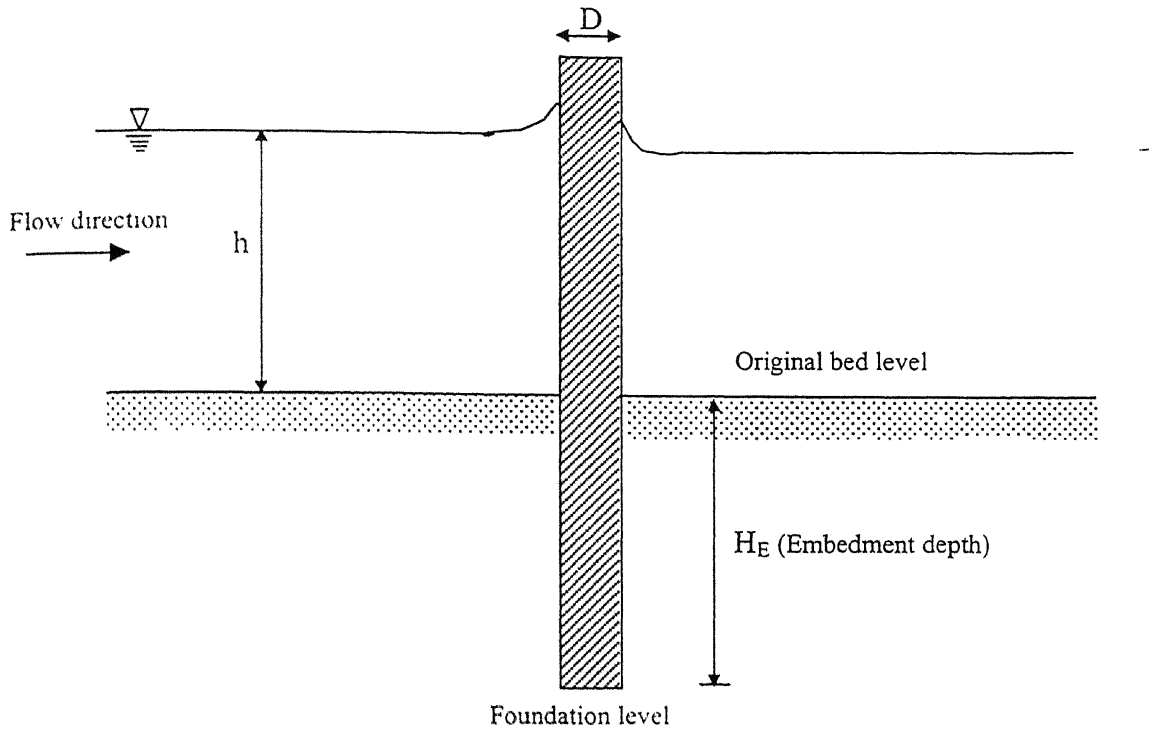

Fig. 2.6 Initial setup of pile before start of scouring

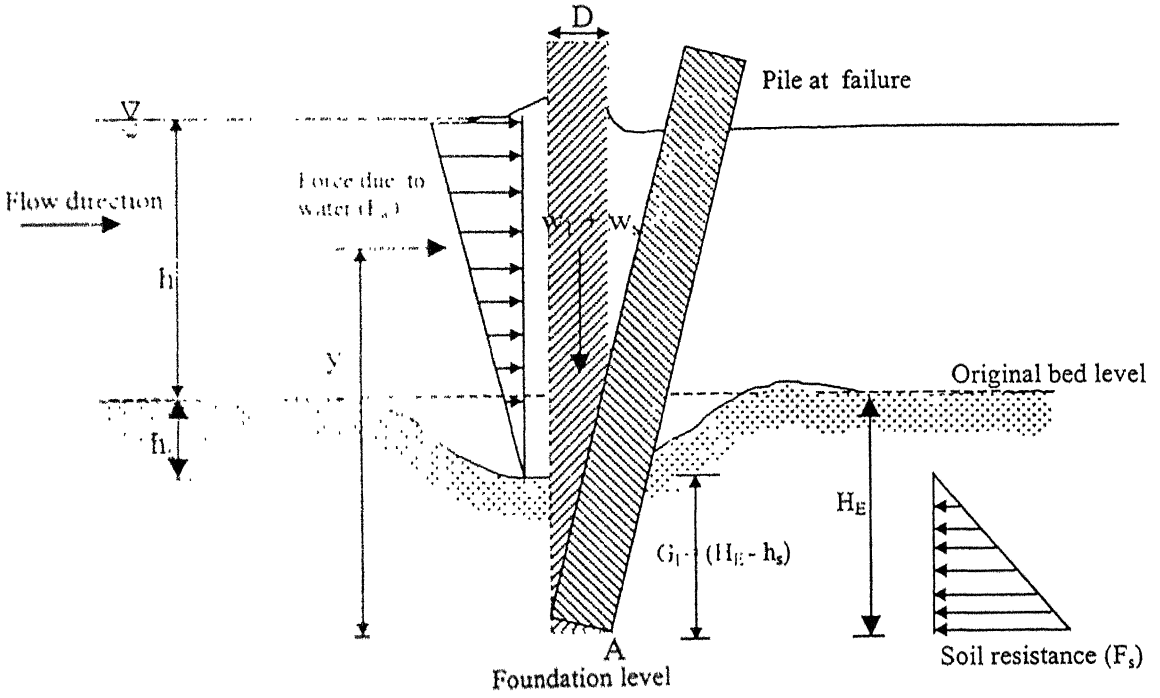

Fig. 2.7 Position of Pile at the time of failure after start of scouring

depth in the case of piles with cap, the pointer of the gauge was bent suitably for accurate measurement of scour depth below the pile cap. After the end of each experiment sediment bed level was properly leveled. Sediments transported by the water current were collected from the trap and put back in the eroded area to get the original bed level.

Chapter III

EXPERIMENTAL RESULTS AND DISCUSSION

In this chapter the data generated through various sets of experiments as discussed and outlined in the previous chapter are presented, analyzed and discussed under different subsections as follows.

3.1 Piles without pile cap

In Fig. 3.1 variation of scour depth ratio (h_s/D) with flow depth ratio (h/D) has been presented. The studies were conducted with a single pile of varying diameters (indicated by different symbols in the diagram), otherwise a wide variation of flow depth ratio (1 to 4) could not be simulated. The study indicates that as the flow depth ratio increases from 1 to 2.2, the scour depth ratio increases, attaining the maximum value of 1.3D at h/D ratio 2.2. There-after, the scour depth ratio decreases with the flow depth ratio. This indicates that up to the limiting value of flow depth ratio (2.2), the strength of horseshoe vortex interaction with the sediment is maximum, resulting in maximum scouring. After the limiting value of h/D=2.2, the strength of the horseshoe vortex may be decreasing with increasing depth of flow manifesting in less scouring effect. This may be explained qualitatively for the distribution of vorticity in the upstream of the pile. The current velocity will be maximum at the surface and zero at the channel bed. As such, vorticity will be maximum at the channel bed and minimum at the surface. Vorticity is significant over a zone, known as wall zone

extending up to 0.2 times the depth of flow (h) for the channel bed. Vorticity of the mean flow in the wall zone wraps up into vortex causing scouring. As the depth of flow increases, the wall zone also increases; however, it can not increase indefinitely and reaches a limiting value beyond which there is no appreciable increase in the vorticity due to viscous effects and channel bed roughness.

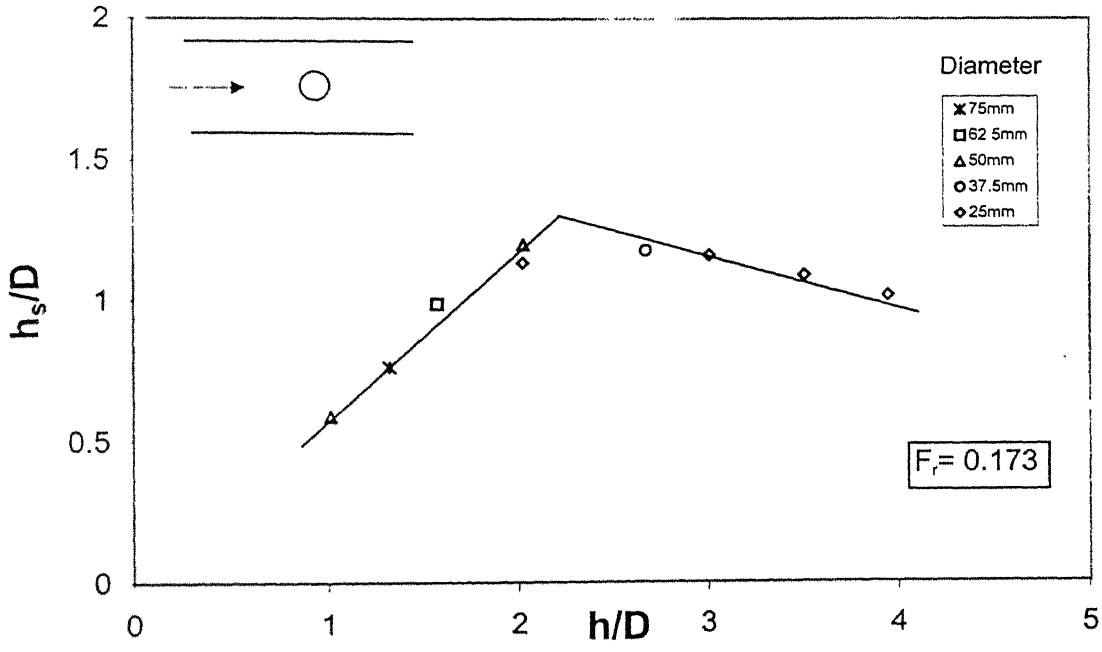

Fig. 3.1 Scour depth variation with flow depth

Studies were made subsequently with two piles arranged in series i.e. the line joining the centers of the two piles is in the direction of flow (tandem pattern) or in parallel (staggard pattern) i.e. flow direction is perpendicular to the line joining the centers of piles. The center to center spacing between the piles was kept as 4D and the piles were designated as P1 and P2. Arrangement of the two piles in series and parallel pattern is shown in Fig. 2.3. It can be seen from the Fig. 3.2, that when the two piles were arranged in series, the relative scour depth around the pile P2 is quite less with respect to the same for pile P1. This is because of the sheltering effect due to the presence of pile P1. But, when the piles are put in parallel, the difference in the values of scour depths has been observed to be quite less. However,

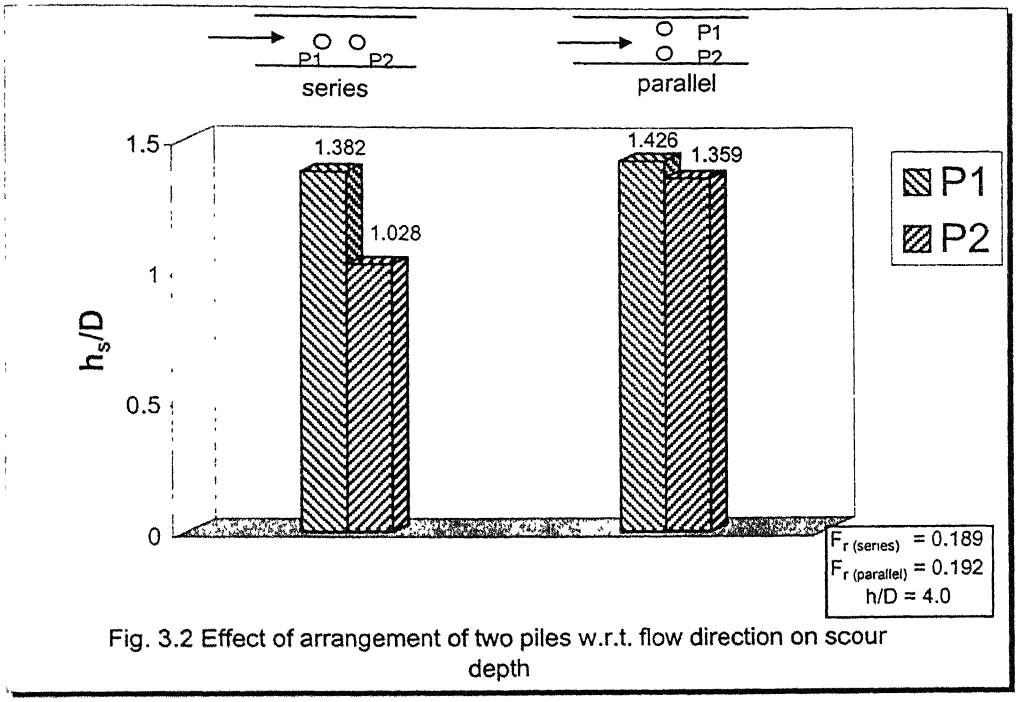

Fig. 3.2 Effect of arrangement of two piles w.r.t. flow direction on scour depth

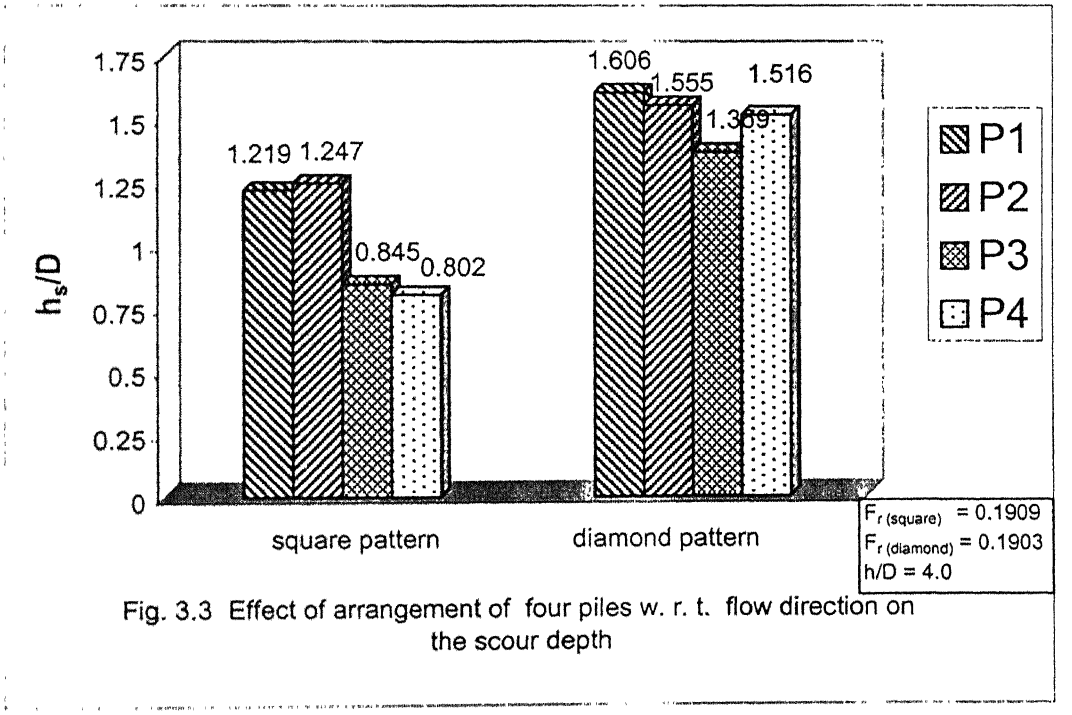

Fig. 3.3 Effect of arrangement of four piles w. r. t. flow direction on the scour depth

intuitively it is felt that there should not be any difference in these values, if the bed conditions around the piles had been the same. The difference might have been caused by non-uniformity of the incoming flow. Similar experiments have been performed with four piles of 25 mm diameter each. In the first series they were kept in a square pattern with a center to center spacing of 4D between piles. Fig. 3.3 shows that for the two front piles, scour depth value comes out to be more than that of the rear piles.

The difference, that have been observed in the scour depth values for the two front piles and the same for the two trailing piles can again be attributed to the same reason as explained earlier.

In the second series of experiments, piles were kept at center to center spacing of 4D between P1 and P2 as well as between P1 and P4 in diamond pattern. It was observed that maximum scouring occurred for the pile P1 and scour depth for P2 and P4 comes out to be nearly the same, where as for the rear pile P3 scour depth decreases considerably due to sheltering effect of piles P1, P2 and P4. These results are also shown in the form of barchart in Fig. 3.3 along with the results for the square pattern of piles.

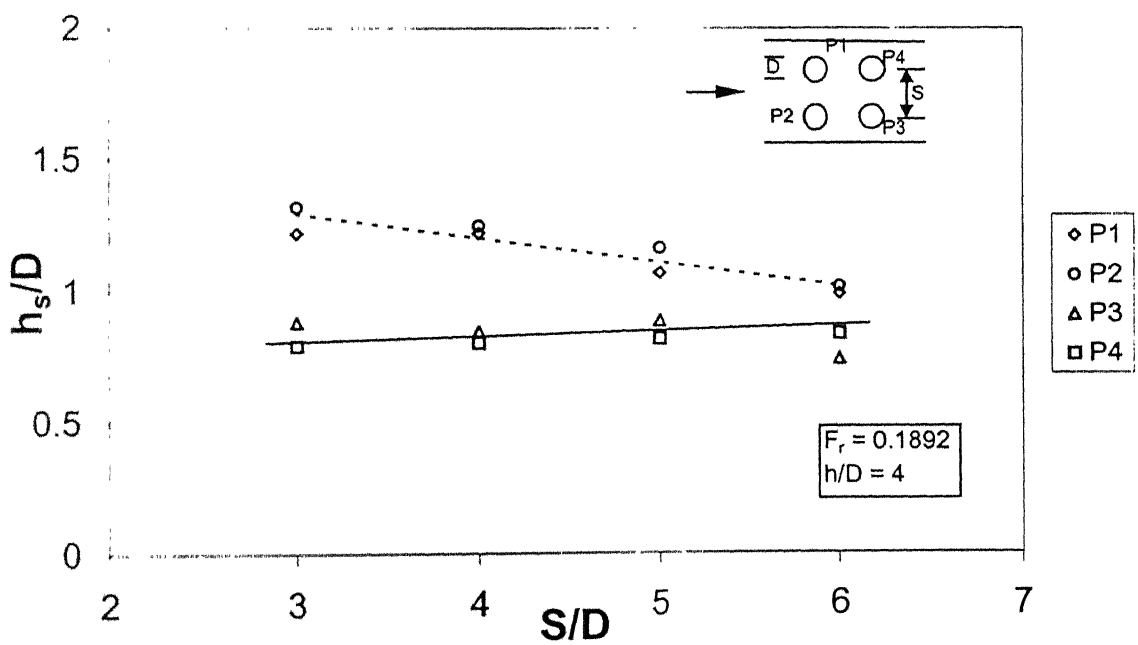

Fig. 3.4 Variation of scour depth with spacing in square pattern

In Fig.3.4 the variation of scour depth with spacing for a group of four piles put in a square pattern, has been shown. It can be seen from the diagram that the erosion is more for the piles P1 and P2, which face the unobstructed flow. Around pile P1 and P2 same amount of erosion is expected. There is little variation in the observed values of scour depth for the piles P1 and P2. However, the difference in the values is not much and is evident from the presented data. Similar observations have been made for pile P3 and pile P4.

From the figure, it can also be concluded that the soil erosion around the rear piles is lesser compared to the same for the frontal piles. As the spacing between piles increases, scour depth decreases gradually with the increase in spacing for the frontal piles, where as for the rear piles scour depth increases gradually. Theoretically beyond certain spacing, both the upstream and downstream piles should experience the same scour. The observed behaviour also corroborates this logic and the same is likely to be achieved for spacing beyond 7. For a given spacing, the ratio of the scour depth for the piles P1 and P2 is maximum, when spacing ratio is 3.

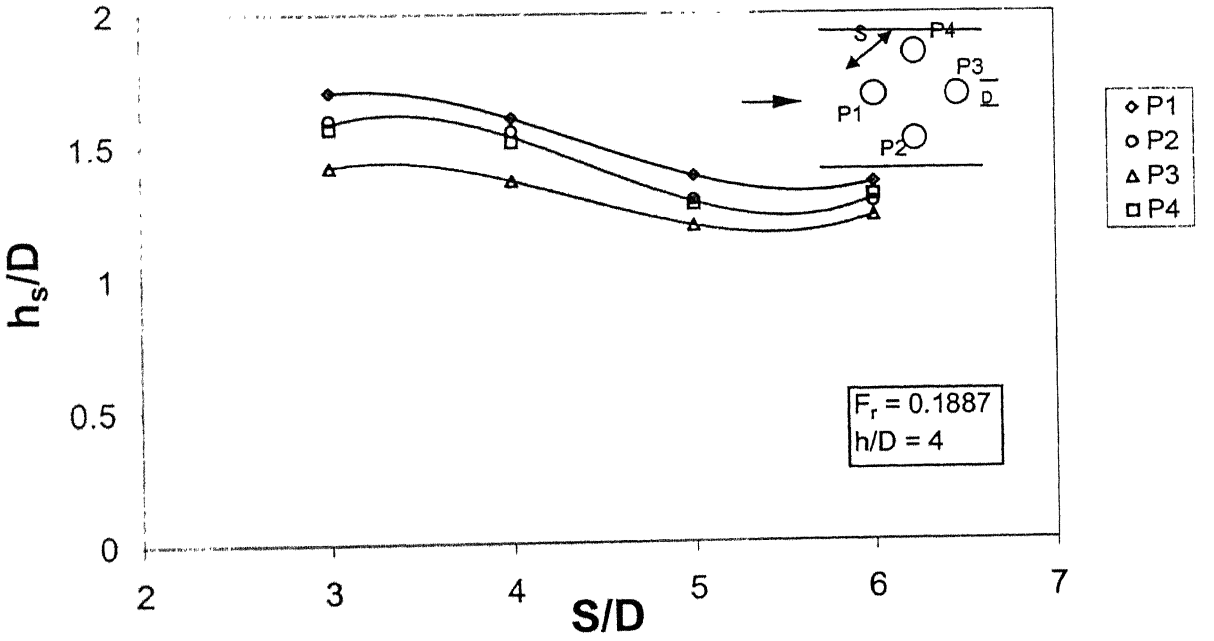

Fig.3.5 Variation of scour depth with spacing in diamond pattern

For the piles arranged in diamond pattern as shown in Fig. 3.5, maximum scour depth is observed around pile P1. As the spacing increases from 3 to 5.5, the scour depth decreases and for spacing greater than 5.5, the scour depth increases very gradually tending to merge to a single value for all the cases. There-after there is no interference effect and each pile will act as an individual pile experiencing same amount of erosion around them. The least scour is observed for the pile P3. The values of scour depth around pile P2 and P4 were same due to all conditions being similar. For square pattern the erosion was maximum for both the frontal piles P1 and P2 but in the diamond pattern maximum erosion occurred only for the pile P1.

Table 3.1 shows the percentage difference between the maximum and minimum scour depths for each pattern and for different spacings of piles. The values have been presented in a non-dimensional form.

Table 3.1 : Maximum and minimum scour depth measurements for four piles arranged in square and diamond pattern

S/D	Scour depth ratios for piles (h_s/D)						%increase in maximum scour depth
	Square pattern			Diamond pattern			
	Maximum	Minimum	% difference	Maximum	Minimum	% difference	
3	1.3175	0.8805	49.63	1.704	1.4212	19.89	29.33
4	1.2467	0.8451	47.52	1.606	1.369	17.31	28.82
5	1.1614	0.985	17.91	1.384	1.1956	15.76	19.17
6	1.143	0.739	54.67	1.356	1.2289	10.34	18.64

It is observed that as the S/D ratio increases for both square and diamond pattern of piles, the maximum and minimum value of scour depth ratio decreases in general. For square pattern, the maximum percentage difference between the maximum and minimum values of scour depth ratio for the entire range of S/D values from 3 to 6 is about 55; Where as for the same, for the diamond pattern is almost 20. The difference in the relative magnitude is more

pronounced in the square pattern as the shielding effect is more for the rear piles in this case than in the diamond pattern.

If one considered the actual value of the scour depth and the benefit accrued to the rear piles due to shielding effect, square pattern of placement of piles should be preferred to the diamond pattern.

In both the cases (square and diamond pattern), maximum scour depth is plotted against spacing between piles, as shown in Fig. 3.6. It is seen that for any spacing the maximum scour depth for diamond pattern comes out to be more than that for the square pattern.

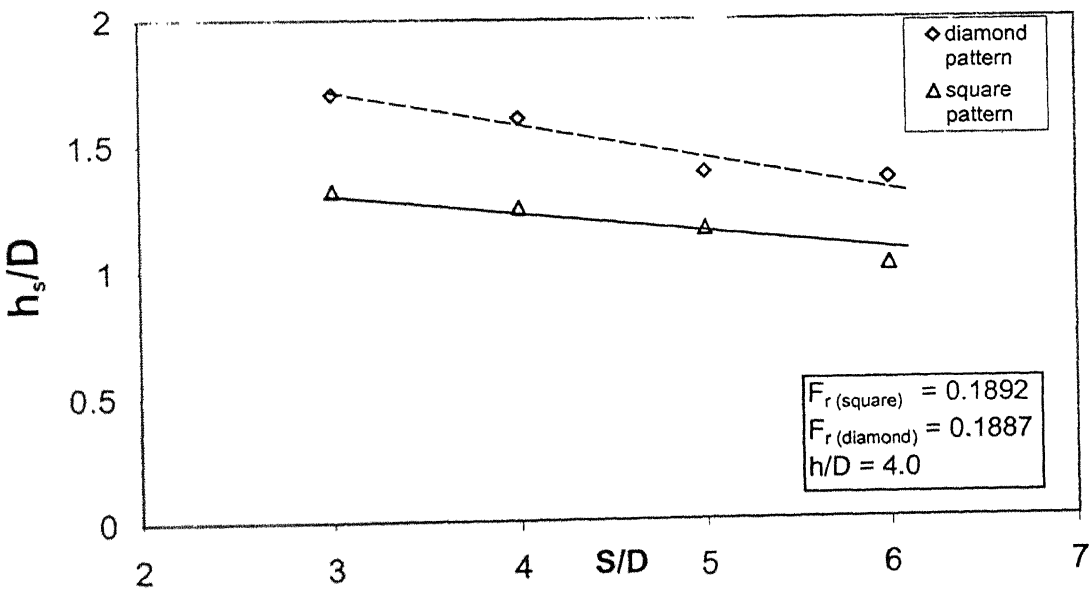

Fig. 3.6 Maximum scour depth vs. spacing for square and diamond patterns

The results are also presented in Fig. 3.7 and Fig. 3.8 in the form of bar charts, when the piles were arranged in square and diamond pattern respectively. In Fig. 3.7, the values of scour depth for the pair of piles (P1 and P2) should be same and so also for the pair P3 and P4. It can be seen that, even though the relative magnitudes were of the same order for these pairs, they were not same as expected. This may be due to the non-uniformity in the flow during the test. In the diamond pattern (Fig. 3.8), scour depth around the piles (P2 and P4) should be identical. Maximum and minimum scour depths could be observed around pile P1 and pile

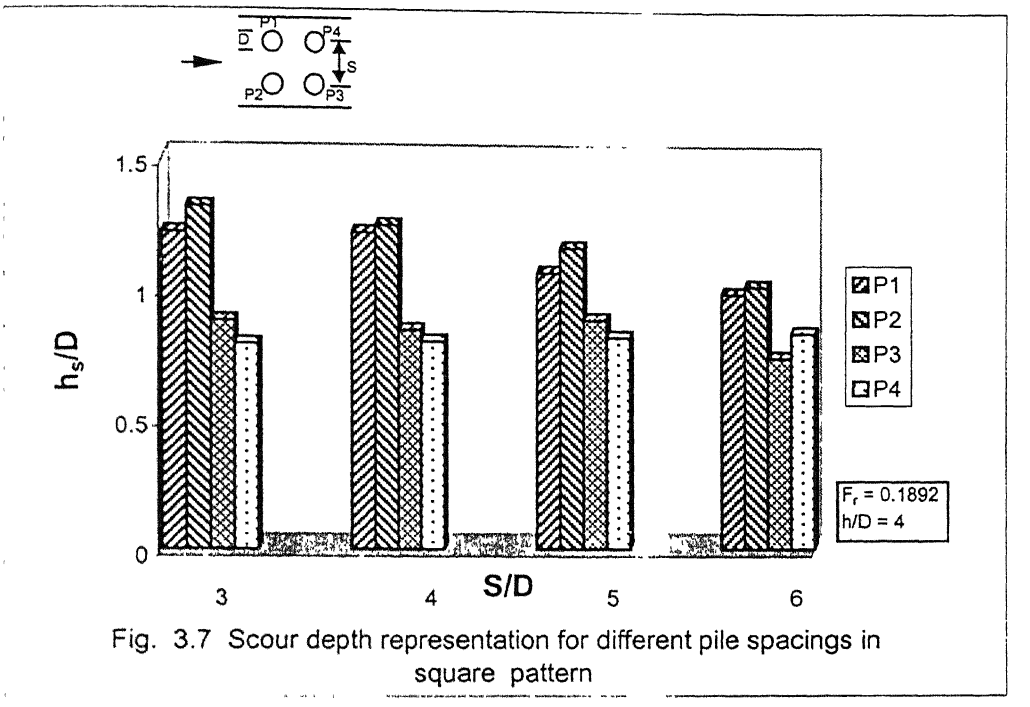

Fig. 3.7 Scour depth representation for different pile spacings in square pattern

P3 respectively with little difference, which may be attributed to the same as stated earlier. The trend of behaviour as observed is expected.

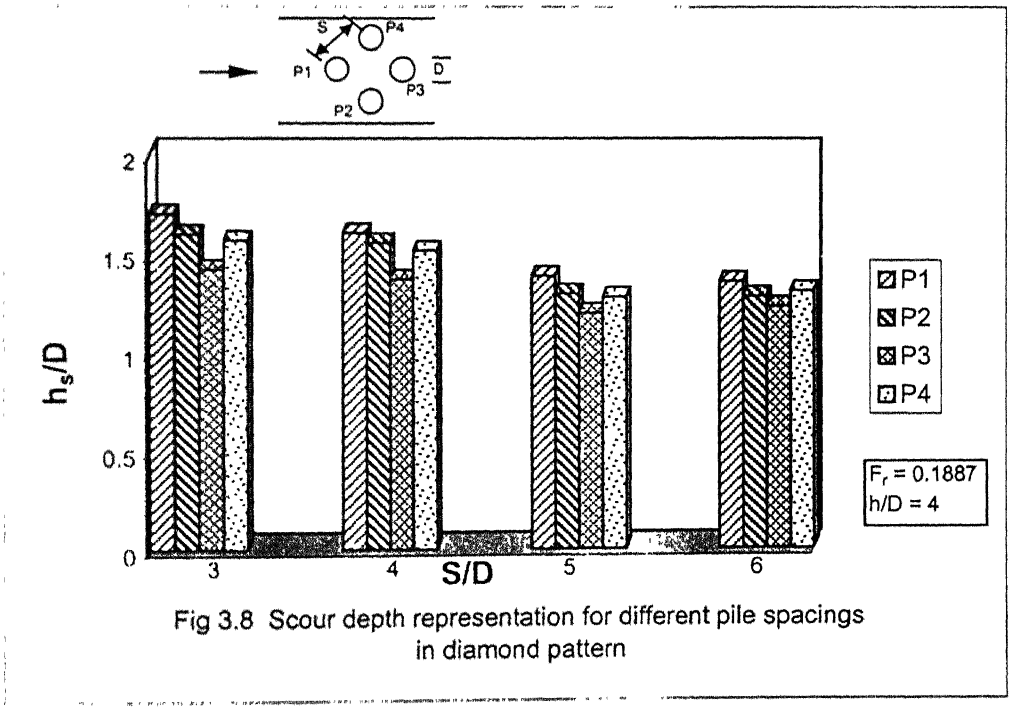

Fig 3.8 Scour depth representation for different pile spacings in diamond pattern

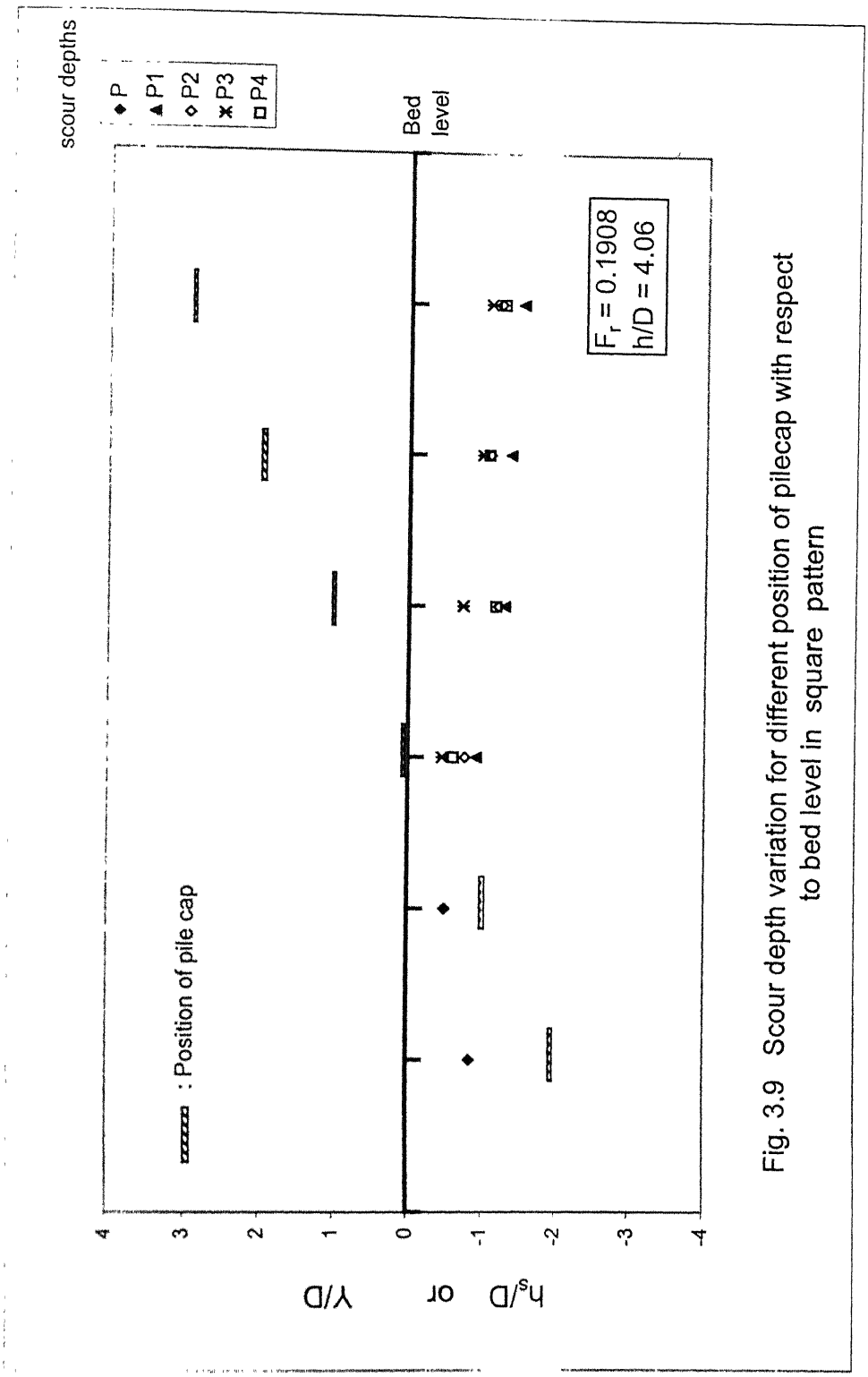

Fig. 3.9 Scour depth variation for different position of pilecap with respect to bed level in square pattern

3.2 Piles with pile cap

In Fig. 3.9 the observed values of scour depth for various arrangement of piles and pile cap are shown. The figure 3.9 also shows the variation of scour depth with the change in the position of pile cap with respect to the bed level. Scour depth for the position of pile cap at Y/D = -2, is due to the scouring around the pier, because top of the pile cap was below the maximum scouring level. When the position of pile cap was at Y/D = -1, scour depth is observed to be the least for any position of pile cap. During this experiment, due to scouring, the top of the pile cap was exposed to flow. It is seen from the observation that this position was quite effective in reducing the local scour depth by interception of the down-flow and arresting of the horseshoe vortex. In the third position, when the pile cap top is rested on the sediment bed level, scour depth again increases as compared to the previous position. Further increase of height of the pile cap from the bed level manifest in the increase in scour depth due to exposure of piles over a greater length to flow and beyond Y/D = 2, there is negligible variation in the scour depth around all the piles.

Similar observations were observed for the diamond pattern and are shown in Fig 3.10. The least scouring is obtained for the position of pile cap at Y/D = -1. Negative sign indicates that it is positioned below the bed level.

Fig. 3.11 and Fig. 3.12, corresponding to both square and diamond patterns respectively showing the variation of scour depth vs time for all the six positions of pile cap (Y/D = -2, -1, 0, 1, 2 and 3 respectively). Scour depth was measured for 600 minutes at different time interval namely 1, 2, 5, 7, 10, 20, 30, 50, 70, 150, 200, 300, 400, 500 and 600 minutes respectively. It is seen that initially scour depth increases with time but thereafter equilibrium stage is reached in most of the cases.

For square pattern the steady state is reached after 60 minutes for Y/D values ranging from -2 to 2. But for Y/D = 3, the trend shows that scour depth still increasing with time indicating that equilibrium state has not yet been attained. The time to reach equilibrium state

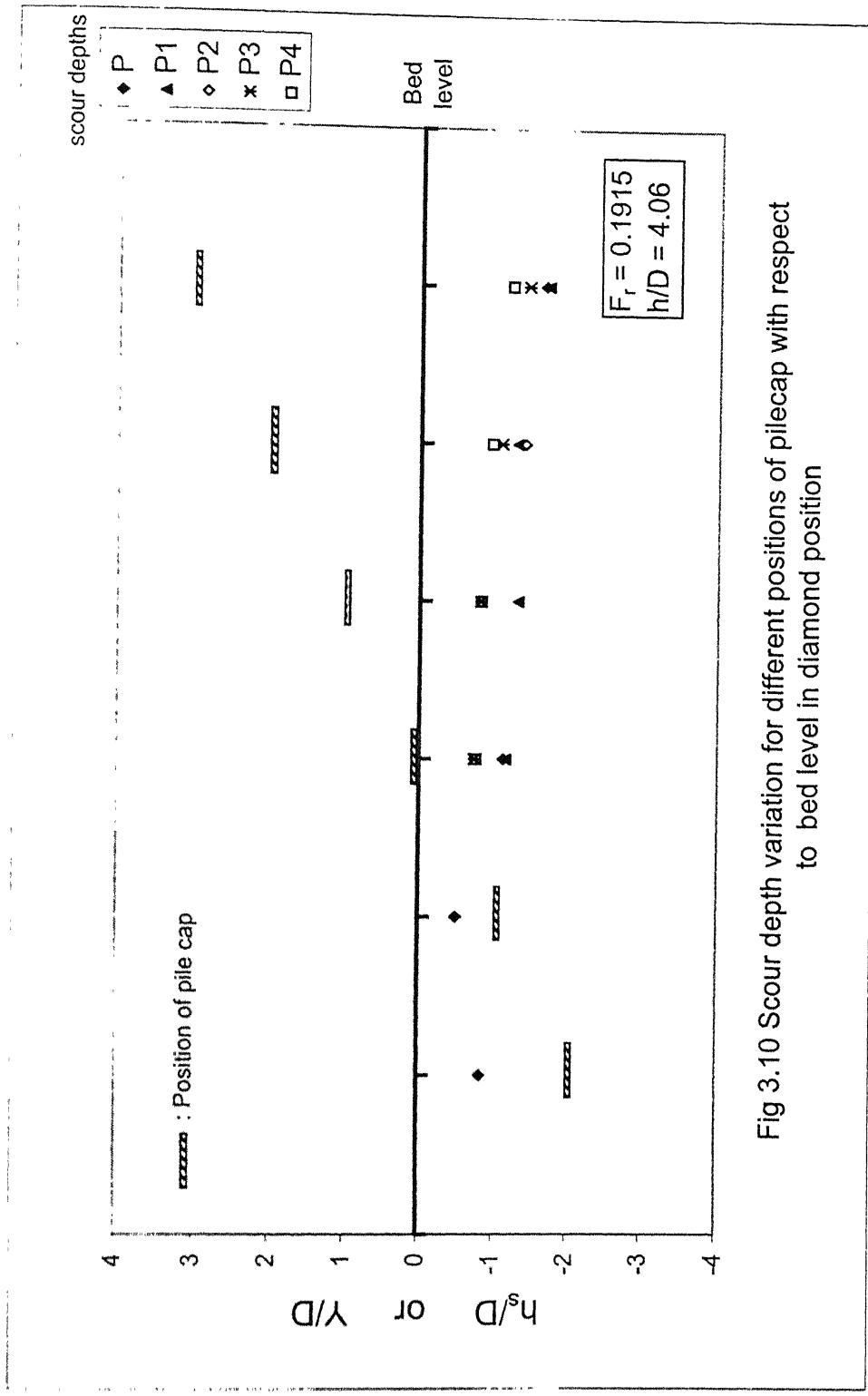

Fig 3.10 Scour depth variation for different positions of pilecap with respect to bed level in diamond position

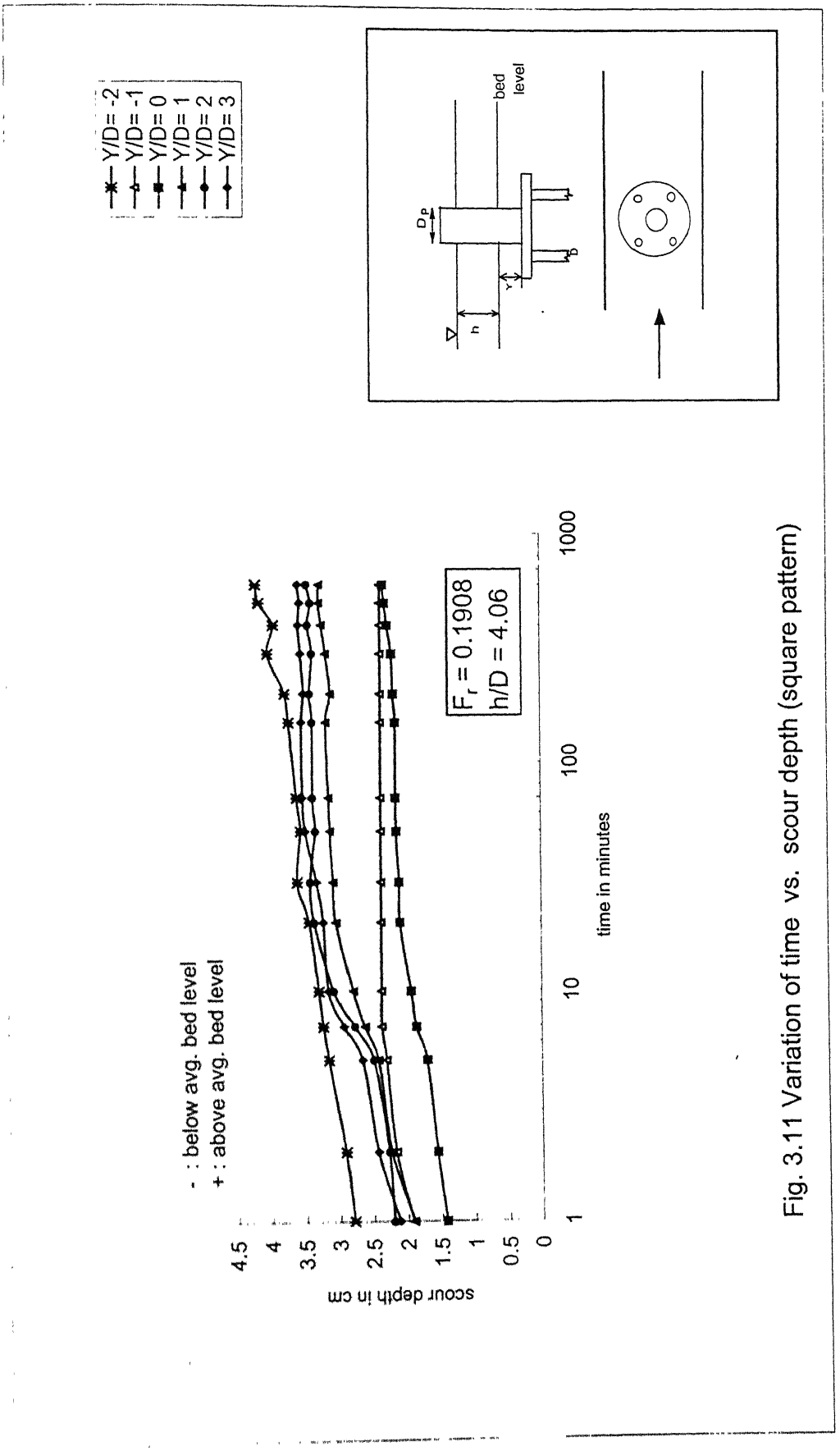

Fig. 3.11 Variation of time vs. scour depth (square pattern)

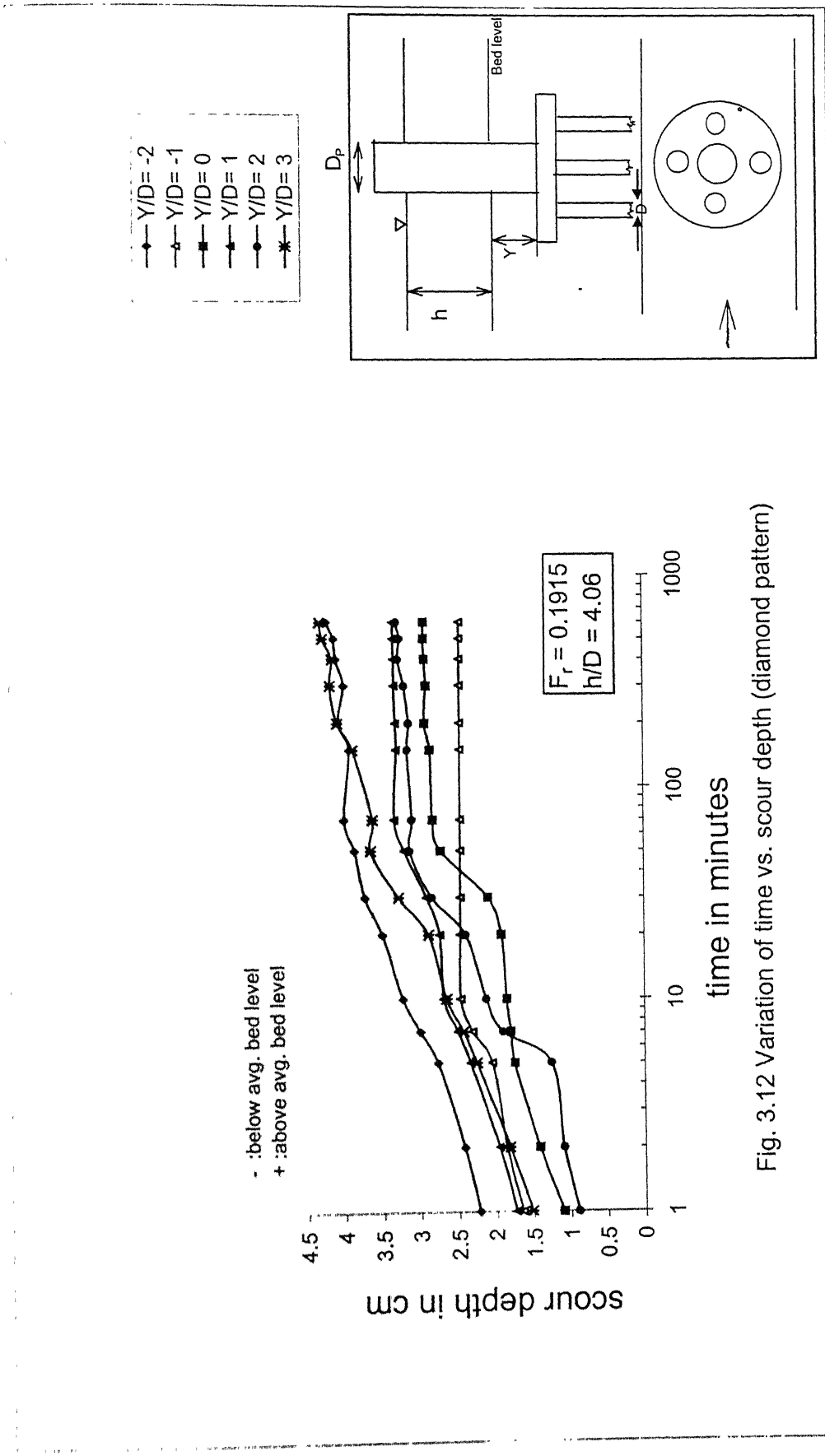

Fig. 3.12 Variation of time vs. scour depth (diamond pattern)

for diamond pattern of piles is about 60 minutes for Y/D ranging from –2 to 1. For Y/D equal to 2 and 3, equilibrium state did dot reach even in 600 minutes.

Table 3.2 Maximum scour depth for different positions of pile cap

Y/D	Max. Scour depth for piles (h_s/D)		% increase in scour depth in diamond pattern w.r. to square pattern
	Square pattern	Diamond pattern	
-2	0.85	0.835	-1.76
-1	0.5	0.5	0.00
0	0.9163	1.1535	25.89
1	1.2894	1.352	4.85
2	1.3602	1.4025	3.11
3	1.5142	1.7	12.27

For different positions of pile cap with respect to bed level, maximum scour depth and percentage increase in scour depth in diamond pattern to that of square pattern is shown in Table 3.2.

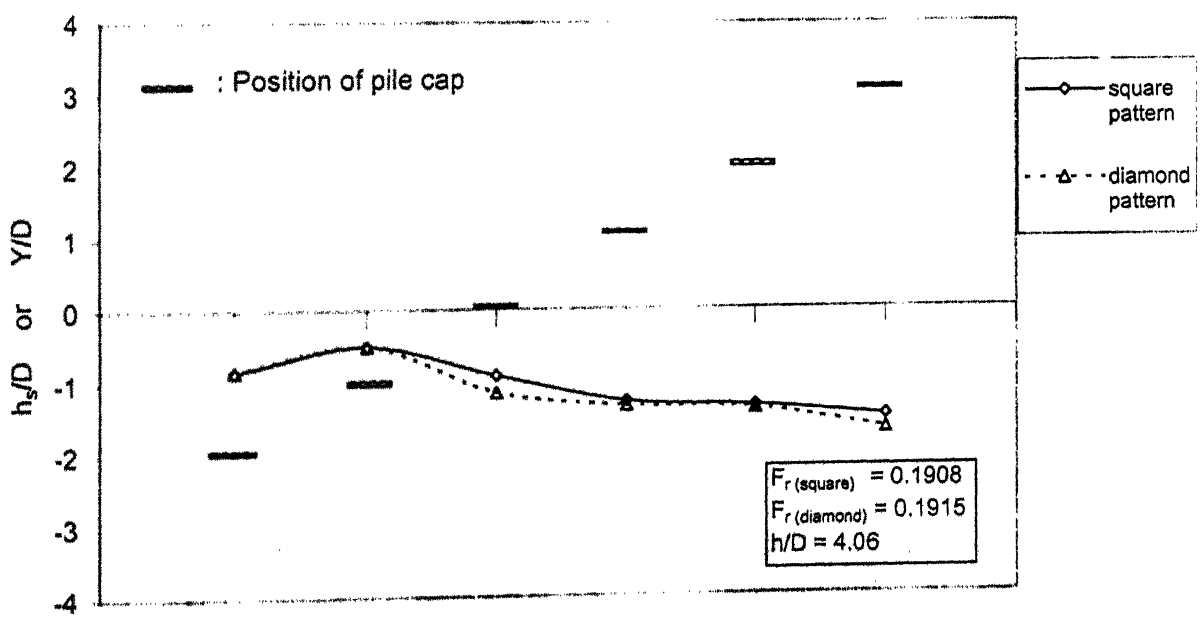

Fig. 3.13 Maximum scour depth for piles with pilecap in different arrangements

Results show that for the pile cap position Y/D = -2 and –1 there is no significant difference in maximum scour depth. At these positions, pier mounted on the pile cap was solely responsible for the local scour.

The values of maximum scour depth for different position of pile cap in both the cases are shown in Fig. 3.13. It can be seen that when Y/D equals to –1, the maximum value of the h_s/D is minimum, signifying the optimum position of the pile cap.

3.3 Variation of scour depth with embedment depth and Froude no.

Fig. 3.14 shows the scour depth data with embedment depth and Froude number. Experimental observations for maximum scour depth corresponding to the limiting equilibrium (incipient failure condition) for various Froude no., flow depth, embedment depth and discharge are given in Table 3.3.

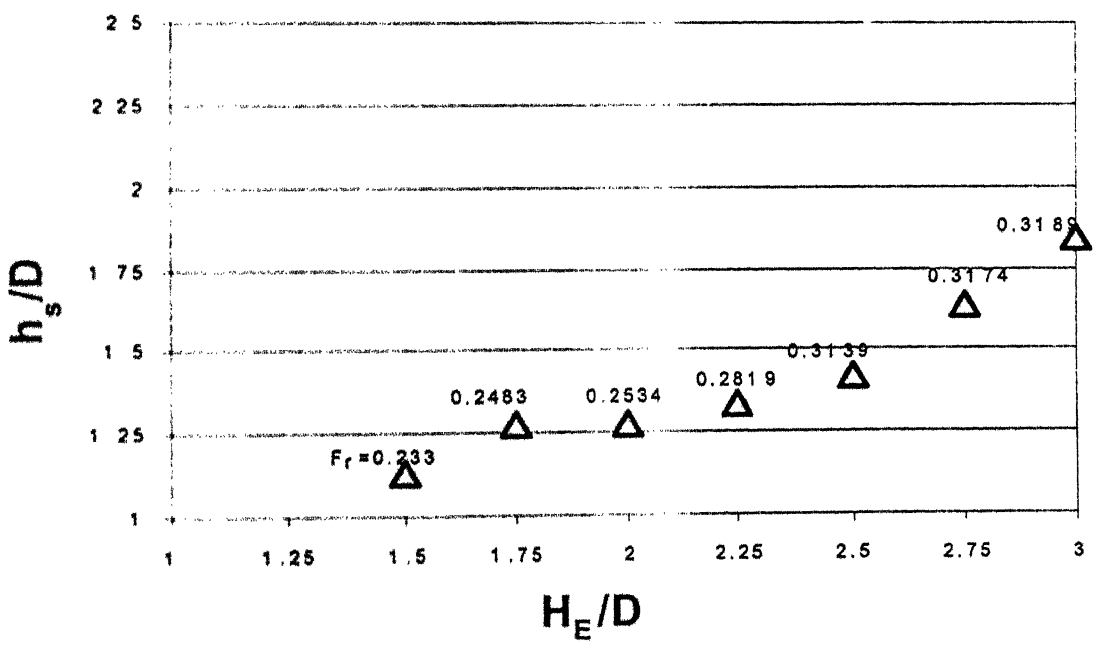

Fig. 3.14 Variation of scour depth with embedment depth and Froude no.

Table 3.3 : Experimental observations for pile at failure condition

S.No.	Embedment depth ratio	Flow depth Ratio	Discharge (q)	velocity	Scour depth ratio	Experiment observations	Froude No. F_r
	H_E/D	h/D	$m^3/sec/m$	m/sec	h_s/D	G_l/D	
1	1.5	2.4713	0.0317	0.2565	1.138	0.362	0.233
2	1.75	2.6333	0.0372	0.2822	1.28	0.47	0.2483
3	2	2.688	0.0391	0.2910	1.276	0.724	0.2534
4	2.25	2.99	0.0510	0.3414	1.34	0.91	0.2819
5	2.5	3.174	0.0687	0.4327	1.42	1.08	0.3174
6	2.75	3.3293	0.0668	0.4011	1.635	1.063	0.3139
7	3	3.3827	0.0695	0.4108	1.846	1.154	0.3189

For meaningful interpretation, experimental observations regarding the Froude number, scour depth ratio and embedment depth ratio are presented in a three dimensional plot in Fig. 3.15. It is observed that there exists a linear relationship among the three parameters.

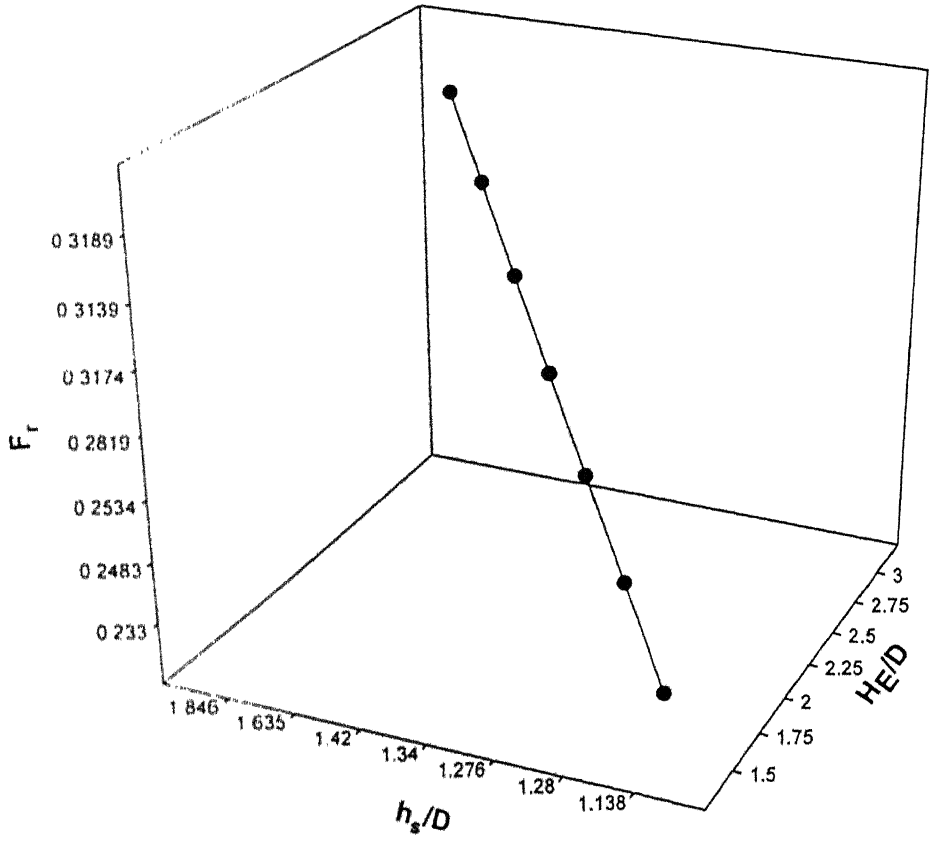

Fig 3 15 3 dimensional model presentation between F_r, H_E/D and h_S/D

Thus a linear relationship between the embedment depth ratio, scour depth ratio and Froude no. is obtained at failure condition by using method of least square as:

$$\frac{h_s}{D} = 0.9173\frac{H_E}{D} - 7.2271F_r + 1.4727$$

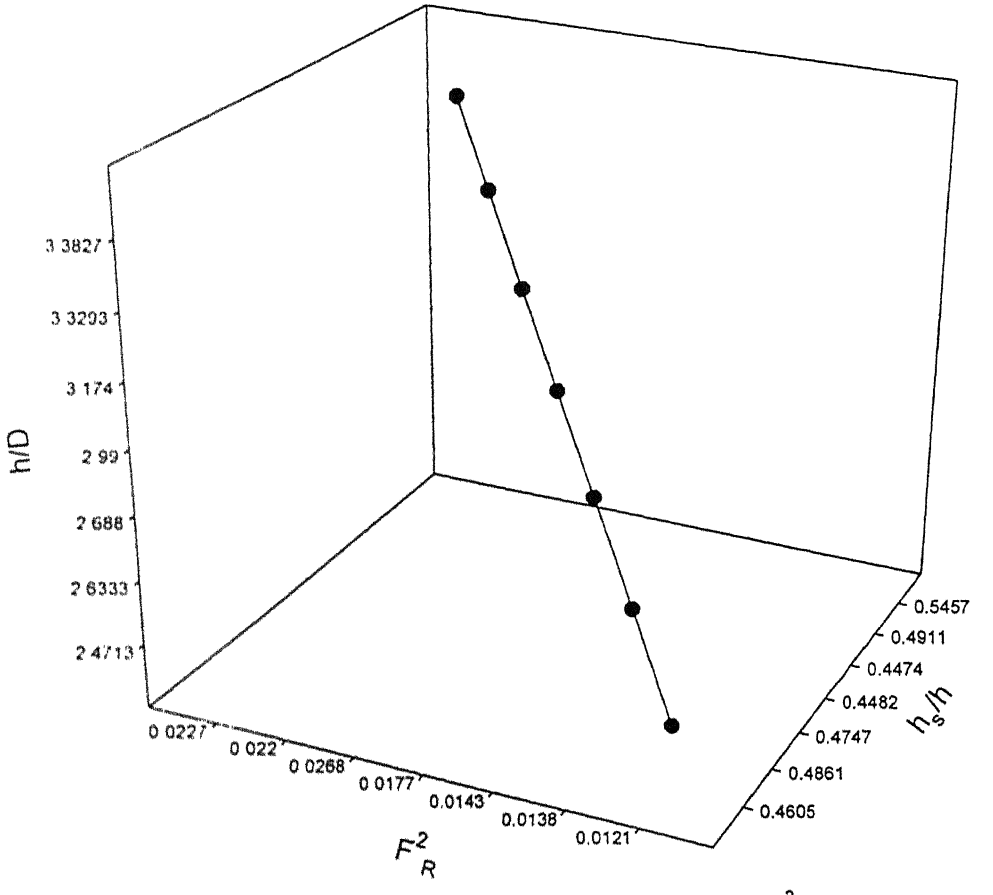

Fig. 3.16: 3-dimensional model presentation between F^2_R, h/D and h_S/h

Similarly Fig. 3.16 shows the three dimensional linear relationship between h_s/h, h/D and F^2_R and relationship obtained among three as follows:

$$\frac{h_s}{h} = 0.1562\frac{h}{D} - 8.3784F_R^2 + 0.1729$$

Using the given relationships, it is possible to predict the scour depth at failure condition corresponding to a given Froude no., embedment depth or flow depth.

-------*------

Chapter IV

THEORETICAL PREDICTION AND COMPARISON WITH EXPERIMENTAL DATA

4.1 General

Embedment depth of piles and piers below the sediment bed level is an important factor for the stability of structures with pile foundation against failure due to overturning caused by the horizontal and lateral forces. Adequate embedment depth imparts resistance against these forces due to wind, water and earthquake etc.

Flow conditions in rivers and other channels may vary due to flood and lead to the significant scouring around bridge piers and piles situated in rivers. Because of scouring,, considerable length of piles is exposed due to erosion of soil on upstream face of the pile facing flow, and thus reduces the grip length of piles, leading to instability of the structure.

Experiments were conducted with different flow conditions, i.e. varying the discharge with the variation of embedment depth below the bed level and maximum scour depth is measured at the point of pile failure (tilted or washed away).

4.2 Theoretical predictive model

A theoretical model has been developed to predict the limiting value of the scour depth at the point of incipient failure.

The assumptions made are as follows:

a. Force due to flowing water acting on the cylindrical pile is assumed to be in a triangular pattern i.e. maximum at the water level and zero at the maximum scouring level.
b. Weight of the pier and load acting over the structure are neglected.
c. Flow conditions are assumed to be uniform through out the experiments.
d. Interference of the walls of the channels are neglected (aspect ratio B/D ≥ 5); where D is the width of pier and B is the width of the channel.

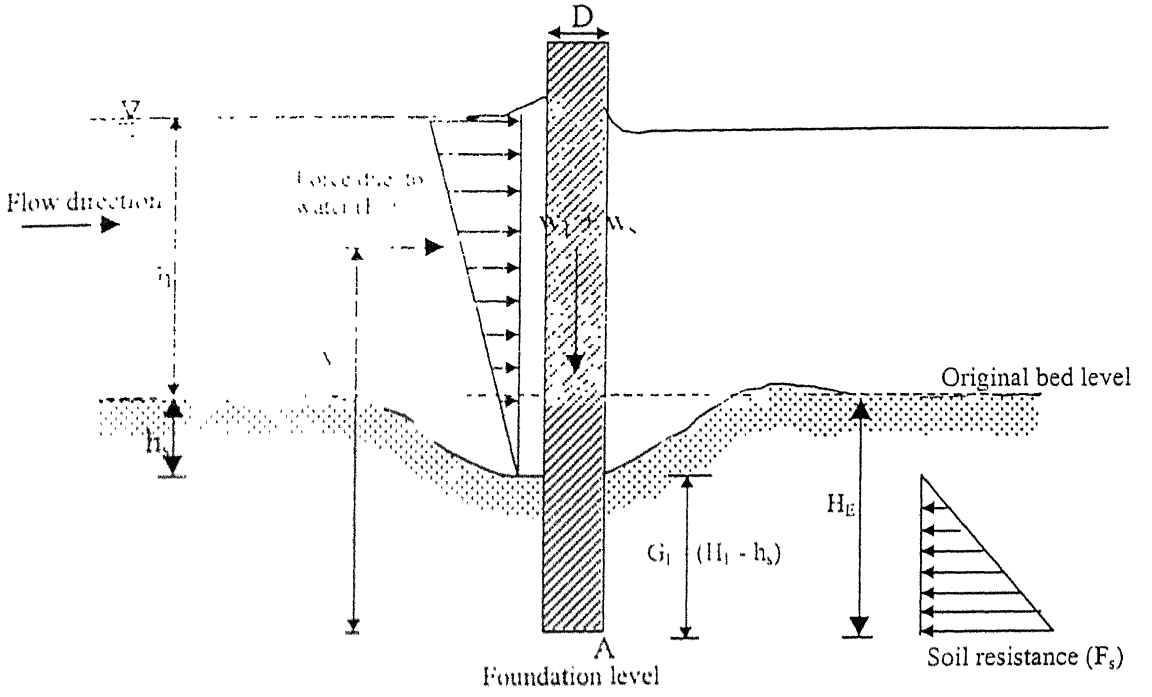

Fig. 4.1 Definition sketch

4.2.1 Derivation

With reference to Fig. 4.1, the different symbols signify the following:

w_l = Weight of the super structure

w_s = Weight of pier

h = Flow depth

h_s = Scour depth

U = Mean velocity of flow

D = Diameter of pile

γ_s' = Submerged density of soil

H_E = Embedment depth of pile below the sediment bed level

y = Distance of F_w from foundation base

G_l = Grip length = $H_E - h_s$

C_D = Drag coefficient

F_R = Modified Froude number

K_p = Coefficient of passive earth pressure

(a) Force due to water current :

$$F_w = \tfrac{1}{2}[\tfrac{1}{2}\rho C_D U^2 D(h + h_s)] \qquad \text{----------(1)}$$

This force is acting from foundation base A at a distance

$$y = [(H_E - h_s) + \tfrac{2}{3}(h + h_s)]$$

(b) Soil resisting force :

Soil resistance F_s is estimated by using Broms's approach (1964) as follows:

$$F_s = \tfrac{1}{2} \times 3\gamma_s' D G_l K_p . G_l$$

$$= \tfrac{3}{2}\gamma_s' D G_l^2 K_p$$

$$= \tfrac{3}{2}\rho_s' g K_p D (H_E - h_s)^2 \qquad \text{----------(2)}$$

This force will act at a distance of $[\frac{G_l}{3} = \frac{1}{3}(H_E - h_s)]$ from the foundation base.

Taking moments of all the forces about the foundation base of pile at point A

$$F_w \times [(H_E - h_s) + \tfrac{2}{3}(h + h_s)] = F_s \times \tfrac{1}{3}(H_E - h_s) + (w_l + w_s)\tfrac{D}{2}$$

Putting the values of F_w and F_s

$$\tfrac{1}{2}[\tfrac{1}{2}\rho C_D U^2 D(h + h_s)][(H_E - h_s) + \tfrac{2}{3}(h + h_s)] = \tfrac{3}{2}\rho_s' g D K_p (H_E - h_s)^2 \tfrac{1}{3}(H_E - h_s) + (w_l + w_s)\tfrac{D}{2}$$

on simplifying, we get:

$$\frac{\rho C_D U^2}{2\rho_s' g K_p} = \frac{[(H_E - h_s)^3 + \frac{(w_1 + w_s)}{\rho_s' g K_p}]}{(h + h_s)[(H_E - h_s) + \frac{2}{3}(h + h_s)]}$$

Let $F_R^2 = \frac{\rho C_D U^2}{2\rho_s' g h K_p}$ and dividing both sides by h, we get-

$$F_R^2 = \frac{[(\frac{H_E - h_s}{h})^3 + \frac{(w_1 + w_s)}{\rho_s' g K_p h^3}]}{(1 + \frac{h_s}{h})[(\frac{H_E - h_s}{h}) + \frac{2}{3}(1 + \frac{h_s}{h})]}$$

since Grip length (G_l) = (H_E-h_s)

$$F_R^2 = \frac{[(\frac{G_l}{h})^3 + \frac{(w_1 + w_s)}{\rho_s' g K_p h^3}]}{(1 + \frac{h_s}{h})[(\frac{G_l}{h}) + \frac{2}{3}(1 + \frac{h_s}{h})]}$$

$$\frac{2}{3}(1 + \frac{h_s}{h})^2 F_R^2 + F_R^2(1 + \frac{h_s}{h})(\frac{G_l}{h}) - [(\frac{G_l}{h})^3 + \frac{(w_1 + w_s)}{\rho_s' g K_p h^3}] = 0 \quad \text{---------- (3)}$$

Solving the above equation, we get-

$$(1 + \frac{h_s}{h}) = \frac{3}{4}[-(\frac{G_l}{h}) \pm \sqrt{(\frac{G_l}{h})^2 + \frac{8}{3}\frac{1}{F_R^2}\{(\frac{G_l}{h})^3 + \frac{(w_1 + w_s)}{\rho_s' g K_p h^3}\}}]$$

Neglecting weight of the pier and superstructure; i.e. w_1 & $w_s \approx 0$, and taking +ve sign:

$$(1 + \frac{h_s}{h}) = \frac{3}{4}[-(\frac{G_l}{h}) + \sqrt{(\frac{G_l}{h})^2 + \frac{8}{3}\frac{1}{F_R^2}(\frac{G_l}{h})^3}] \quad \text{---------- (4)}$$

Since from the experimental observations, relationship between h_s/h , F_r and H_E/D obtained from the theory of least error is as follows :

$$\frac{h_s}{h} = 0.1562(\frac{h}{D}) - 8.3784F_R^2 + 0.179 \quad \text{---------- (5)}$$

substituting the value of h_s/h in equation (4):

$$1.179+0.1562(\frac{h}{D})-8.3784F_R^2=\frac{3}{4}[-(\frac{G_l}{h})+\sqrt{(\frac{G_l}{h})^2+\frac{8}{3}\frac{1}{F_R^2}(\frac{G_l}{h})^3}] \quad \text{---------- (6)}$$

let :

$$a=\frac{4}{3}[1.179+0.1562(\frac{h}{D})-8.3784F_R^2],\ b=\frac{8}{3}\frac{1}{F_R^2}$$

and $G_l/h = x$

now equation (6) can be expressed as:

$$a=[-x+\sqrt{x^2+bx^3}]$$

$$1+\frac{a}{x}=\sqrt{1+bx}$$

squaring and simplifying the above equation:

$$x^3+(-\frac{2a}{b})x+(-\frac{a^2}{b})=0 \quad \text{----------(7)}$$

which is in the form of polynomial of third degree. Solving the above equation by using Cardan's algorithm, we get the roots of the above equation, which corresponds to the theoretically predicted values of G_l/h.

Table 4.1 : Experimental observations and theoretical predictions

S.No. (1)	Embedment depth ratio (2)	Flow depth Ratio (3)	Scour depth ratio (4)	Froude No. (5)	Experiment observations (6)	Theoretical prediction (7)	Goodness ratio 7÷6
	H_E/D	h/D	h_s/D	F_r	$(G_l/h)_e$	$(G_l/h)_t$	
1	1.5	2.4713	1.138	0.233	0.1465	0.2807	1.92
2	1.75	2.6333	1.28	0.2483	0.1785	0.2952	1.65
3	2	2.688	1.276	0.2534	0.2693	0.3002	1.12
4	2.25	2.99	1.34	0.2819	0.3043	0.3269	1.07
5	2.5	3.174	1.42	0.3174	0.3403	0.3726	1.09
6	2.75	3.3293	1.635	0.3139	0.3349	0.3562	1.06
7	3	3.3827	1.846	0.3189	0.3412	0.3607	1.06

4.3 Results and Discussion

Using the above expression (eq. 7), the values of ratio G_l/h are computed for different h/D, h_s/D, H_E/D and F_1 values. The computed values are presented in Table 4.1. In the same table, the corresponding values as observed in the laboratory are also presented. The correctness of predicted values of grip length ratio (G_l/h) with respect to the experimental observations is measured in terms of a Goodness ratio defined as the ratio of the theoretical prediction of the same to the experimentally observed values. The values of Goodness ratio as shown in Table 4.1 are very close to unity for embedment depth ratio (H_l/D) greater than 2. For embedment depth ratio greater or equal to 2.25 but less than 3, the Goodness ratio ranges from 1.06 to 1.09. Even for grip length ratio equal to 2, the Goodness ratio 1.12 gives an error, which for all practical purpose can be considered to be with in the range of possible experimental error. Thus, the proposed semi-empirical theory can be used for predicting the grip length with confidence with in this range (H_E/D= 2 to 3). But, for H_l/D less than 2, the use of the theory gives large error. So it should not be used for H_E/D values less than 2. Thus, it is necessary to make an effort to improve the theory, so that it can be applied for a large range of H_E/D values.

Chapter V

CONCLUSIONS

5.1 General

In the present study, investigations have been carried out under three phases. In the first phase experiments were conducted with isolated piles (with out pile cap) simulating the conditions of foundations of river crossing foundations under different flow conditions and their arrangement in a group. This study helps in finding out the relative equilibrium scour depth of piles in a group and their suitable arrangement in a group as a whole to get the least erosion around the piles.

In phase two, experimental were focussed on the study of piles with a pilecap and a pier mounted on the top. Experimental observations reveal the suitable position of pilecap with respect to the sediment bed level and arrangement of piles in a group. Variation of equilibrium scour depth with time is measured for each set of experiment.

In the third and last series, practical aspect of pier failure with the variation of embedment depth of it below the bed level with Froude number, scour depth and flow depth was studied. On the basis of experimental and theoretical predictive models, relationships are developed for the above mentioned parameters.

The major conclusions of all phases of the study are as follows:

5.2 Piles with out pile cap:

(a) Experiments for the individual piles facing flow, show that scour depth ratio (h_s/D) increases initially with flow depth ratio (h/D) and attains the maximum value at h/D = 2.2; beyond the limiting value (2.2) scour depth ratio decreases as the flow depth ratio increases.

(b) Arrangement of two piles arranged in series and in parallel pattern shows that, in series arrangement, scour depth for rear pile is quite less (around 35%) than that for the front pile due to the sheltering effect. In parallel arrangement, equilibrium scour depth for both the piles comes out to be almost same.

(c) Observations for four piles arranged in a square and diamond pattern show that, when the piles are placed in a square pattern, scour depth values for the front two piles facing flow are more than that for the rear two piles. Results obtained for the piles arranged in diamond pattern show that maximum scouring occurs for the front most pile P1 and almost same scour depths for the piles P2 and P4. Least scouring occurs for the pile P3, which may be attributed to the sheltering effect of the rest of the three piles.

(d) Variation of scour depth with c/c spacing between piles arranged in square and diamond pattern show that in the square pattern, as the spacing increases, scour depth decreases for the frontal piles and for the rear piles scour depth increases gradually with the increase in spacing.

In diamond pattern, maximum scour depth is observed for the pile P1 for all spacing ratios ranging from 3 to 6. Scour depth ratio decreases as spacing ratio increases from 3 to 5.5 and beyond spacing ratio 5.5 scour depth increases gradually tending to merge at a single value.

Comparison of above observations in both the arrangements show that for any spacing ratio, maximum scour depth for diamond pattern comes out to be more than that for the square pattern. Thus, square arrangement of piles is preferable to that of diamond pattern.

5.3 Piles with pile cap:

(a) From the experimental observations it is concluded that minimum scour depth occurs when the pile cap is placed at a depth equivalent to the diameter of the pile below the sediment bed level.

(b) In all six set up of experiments i.e. for pile cap positions Y/D=-2, -1, 0, 1, 2 and 3; results show that scour depth values were observed similar for the pile cap positions Y/D= -2 & 1 in square and diamond pattern, while for the rest positions of pile cap i.e. at Y/D= 0, 1, 2 and 3; diamond pattern shows more scouring values than that in square pattern of piles.

5.4 Theoretical predictions:

The developed theoretical model for predicting the grip length is found to be more reliable for embedment ratio greater than 2. The predictions made using the developed model matches excellently with those experimentally observed.

5.5 Suggestion for the further studies :

Based on the present work on Yamuna sand (d_{50} = 0.60 mm), the following aspects of work are suggested for further studies:

1. All the findings related to the mechanism of scour and least scour arrangements of piles should be tried for different sediments and a comparative study can be made.
2. Present study may be focussed towards the scouring pattern in stratified soil deposits.
3. Apart from square and diamond pattern of piles, another alternative arrangements of piles to get minimum scouring around piles in a group can be studied.

REFERENCES

- Baker, C. J. (1981), "New Design Equation for scour around Bridge Piers", Jr. of Hydraulic Division, Proc. ASCE, Vol. 107 (HY-4)
- Baker, R. E. (1986), "Local Scour at Bridge Piers in Non-uniform sediment", Rep. No. 402, School of Engg., The University of Auckland, New Zealand.
- Barnard, S. and Child, J. M. (1994), "Higher Algebra", Macmillan Publishers, pp.-180.
- Breusers, H.N.C., Nicollet, G., and Shen, H.W. (1977), "Local Scour around Cylindrical Piers", J. Hydr. Res., Vol. 15(3) : 211-252.
- Chiew, Y.M. (1984), "Local Scour at Bridge Piers", Ph.D. Thesis, The Univ. of Auckland, Auckland, New Zealand.
- Dongal, D.M.S. (1994), "Local Scour at Bridge Abutments", Rep. No. 544, School of Engg., The Univ. of Auckland, New Zealand.
- Ettema, R. (1980), "Scour at Bridge Sites", Rep. No. 117, Univ. of Auckland, Auckland, New Zealand.
- Jones et al. (1993), "Preliminary Studies of Pressure Flow Scour", ASCE Hydraulic Engg., Proc. National conference, San Francisco.
- Kothyari, U.C. (1989), "Scour Around Bridge Piers", Ph.D. Thesis, Univ. of Roorkee, India.
- Laursen, E. M. and Toch, A. (1956), "Scour Around Bridge Piers and Abutments", Iowa Highway Res. Board, Bulletin No.4, pp. 60.
- Laursen, E. M. (1963), "Analysis off Bridge Scour", J. Hydr. Div., ASCE, Vol. 89 (3), 93-118.
- Melville, B.W. (1997), 'Pier and Abutment Scouring : Integrated Approach", Jr. Hydr. Engg., ASCE, Vol. 123 (2) : 125-135
- Melville, B.W. (1998), "Effects of Pier Shape On Local Scour", Jr. of Water Resource Engg., ASCE.
- Melville, B.W. (1992), "Local Scour at Bridge Abutment", Jr. Hydr. Engg., Proc. ASCE, Vol. 118 (4) : 615-631.

- Melville, B.W. (1975), "Local Scour at Bridge Sites", Rep. No. 117, Univ. of Auckland, Auckland, New Zealand.
- Melville, B.W. (1988), "Scour at Bridge Sites", Chapter 15, Civil Engineering Practice, Ed. P.N. Cheremisinoft, San Ling Chang.
- Muzzammil, M. and Gangadharaiah, T. (1995), "A Study of Scouring Horseshoe Vortex", 6th International Symposium in River Sedimentation, New Delhi, Nov. 7-11 : 923-943.
- Raudkivi, A.J., and Ettema, R. (1977), "Effect of Sediment Gradation on Clear Water Scour", Jr. Hydr. Div., ASCE, Vol. 103 (10) : 1209-1212.
- Raudviki, A. J. (1990), "Loose Boundary Hydraulics", Pergamon Press.
- Setia, B. (1997), "Scour Around Bridge Piers : Mechanism and Protection", Ph.D. Thesis, Indian Institute of Technology, Kanpur.
- Shen, H.W., Schneider, V.R. and Karaki, S. (1969), "Local Scour Around Bridge Piers", Jr. Hydr. Div., ASCE, Vol. 95 (6) : 1920-1940.
- Sheppard, D.M. and Jones, J.S. (1998), "Scour at Complex Pier Geometries", Jr. of Water Resource Engg., ASCE.
- Wong, W. H. (1982), "Scour at Bridge Abutments", Masters Thesis, University of Auckland, Report No. 275.

APPENDICES

APPENDIX

(A) Experimental observations for piles with out pile cap

Table A1 : Scour depth variation with flow depth

H (mm)	h/D	h_s (mm)	h_s/D	Dia. of model (mm)	F_r
50.6	1.012	29.4	0.588	50	0.1582
50.625	2.025	28.3	1.132	25	0.1419
75.23	3.009	28.97	1.1588	25	0.1493
87.85	3.514	27.165	1.0866	25	0.1657
98.8	3.952	25.39	1.0157	25	0.1863
98.9	1.3187	57.15	0.762	75	0.1865
99.8	1.5968	61.71	0.9874	62.5	0.1882
100 19	2.6717	44.06	1.175	37.5	0 1889
101 4	2 028	59.925	1.1985	50	0.1912

Table A2 : Two piles in series and parallel pattern

Diameter of piles (D) : 25 mm

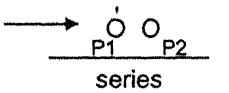

series

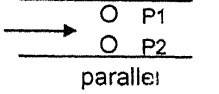

parallel

pattern	h (cm)	h/D	Scour depth ratio h_s/D		Froude no. (F_r)	c/c spacing
			P1	P2		
series	10.013	4.0052	1.382	1.0275	0.1888	4D
parallel	10.195	4.078	1.426	1.359	0.1922	4D

Table A3 : Variation of scour depth with c/c spacings of four piles arranged in sqaure pattern

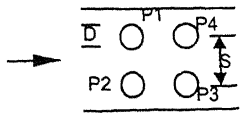

Diameter of piles (D) : 25 mm

Spacing ratio (S/D)	h (mm)	h/D	Scour depth ratio (h_s/D)				F_r
			P1	P2	P3	P4	
3	100.07	4.0028	1.2189	1.3175	0.8805	0.7913	0.1887
4	101.26	4.0502	1.2192	1.2467	0.8451	0.802	0.1909
5	100.47	4.0186	1.0669	1.1614	0.885	0.8175	0.1894
6	99.57	3.9823	0.9855	1.0143	0.739	0.835	0.1877

Table A4 : Variation of scour depth with c/c spacings of four piles arranged in diamond pattern

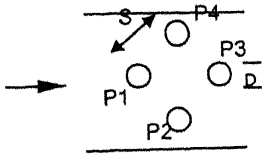

Diameter of piles (D): 25 mm

Spacing ratio (S/D)	h (mm)	h/D	Scour depth ratio (h_s/D)				F_r
			P1	P2	P3	P4	
3	99.3	3.972	1.7039	1.5996	1.4212	1.5681	0.1872
4	100.9	4.036	1.606	1.555	1.369	1.5157	0.1903
5	98 6	3.944	1.384	1.2938	1.1956	1.2769	0.1859
6	101.6	4.064	1.356	1.2808	1.2289	1.3088	0.1916

(B) Experimental observations for piles with pile cap in a square pattern :

Diameter of piles (D): 25 mm
Diameter of the pier on top of the pilecap (D_P): 50 mm
Thickness of the pilecap : 12 mm
Diameter of pilecap : 150 mm

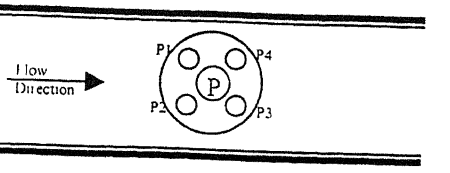

Table B1 : Scour and flow depth observations

Position of pilecap (Y/D)	h (mm)	h/D	Scour depth ratio (h_s/D)					F_r
			P	P1	P2	P3	P4	
-2	101.73	4.069	0.845	-	-	-	-	0.1918
-1	100.5	4.02	0.5	-	-	-	-	0.1895
0	101.8	4.072	-	0.9163	0.7628	0.4588	0.6014	0.1920
1	101.63	4.065	-	1.2894	1.2027	0.7303	1.1634	0.1916
2	100.21	4.082	-	1.3602	1.0876	0.9852	1.0639	0.1924
3	101.2	4.048	-	1.5142	1.2145	1.0846	1.2539	0.1908

Table B2 : Variation of time vs. scour depth for different positions of pile cap

Time in Minutes	scour depth (h_s) in cm					
	Y/D= -2	Y/D= -1	Y/D=0	Y/D=1	Y/D=2	Y/D=3
1	2.7925	1.92	1.4275	1.905	2.205	2.1225
2	2.9125	2.165	1.5575	2.235	2.275	2.4325
5	3.1525	2.295	1.6975	2.415	2.485	2.6525
7	3.2325	2.365	1.8575	2.615	2.765	2.9225
10	3.2925	2.365	1.9275	2.785	3.075	3.1526
20	3.4325	2.365	2.0875	3.035	3.355	3.2225
30	3.6025	2.365	2.0975	3.075	3.415	3.3225
50	3.5525	2.365	2.1375	3.115	3.335	3.4825
70	3.6125	2.365	2.1475	3.135	3.375	3.5225
150	3.7225	2.365	2.1475	3.175	3.375	3.5325
200	3.7825	2.365	2.1775	3.105	3.415	3.5025
300	4.025	2.365	2.1975	3.175	3.375	3.5425
400	3.942	2.365	2.2575	3.235	3.435	3.5725
500	4.1525	2.365	2.2975	3.275	3.395	3.5525
600	4.2023	2.365	2.3275	3.275	3.455	3.5825